17 June 2006

AMMA-EU Project: Deliverable 1.1.2a

Preliminary Estimates of the Impact of West African Emissions on Global Trace Gas and Aerosol Budgets – Identification of Model Uncertainties

Contributors:

LMDz-INCA: Idir Bouarar, Mai Pham, Kathy Law (CNRS-IPSL-SA)
TM4: Twan van de Noije (KNMI)
MOCAGE: Jean-Luc Attie (CNRS-LA), Vincent-Henri Peuch, Bernadette Josse (CNRM)
TM4-ORISAM: Cathy Liousse (CNRS-LA)
MODIS analysis: Didier Tanré (CNRS-LOA)

1. Introduction and Background

A major goal of the AMMA project is to improve predictions of climate on seasonal and multi-annual timescales using coupled atmosphere-ocean or chemistry-aerosol climate models. This requires improved understanding about the processes that govern chemical composition over West Africa. As a first step towards these aims, this report summarises recent evaluations of global chemistry and aerosol models against data. This provides information on model uncertainties and identifies which processes should be investigated in more detail. As such, this report provides input into WP2.4 that focuses on detailed studies of processes influencing trace gases and aerosols and will make use of data collected during the SOPs. It is also linked to work in 4.1.3 on more detailed comparison of particular processes in different scale models.

Here, we assess model simulations of trace gases and aerosols. Correct simulation of distributions of these constituents depends on many factors. For trace gases, the main trace gas of interest is ozone (O_3) which can influence regional and global climate as well as local air quality. Its distribution over West Africa depends on emissions of precursors (NO_x, CO, VOCs), transport processes (PBL exchange, deep convection, advection, stratospheric flux), and loss processes affecting O_3 itself (dry deposition, chemical reactions). Aerosols over West Africa include mineral dust, black carbon, primary organic carbon and secondary organic aerosols produced from biogenic emissions.

Emissions of O_3 precursors and aerosols come from a wide variety of sources. Biomass burning is a key contributor to NO_x, CO and black carbon emissions over West Africa and is highly seasonal with a maximum in the dry season (Nov-Mar). Anthropogenic emissions are also an important source of carbonaceous aerosols, CO, VOCs, and possibly, NO_x close to large cities such as Lagos although their magnitude is very uncertain over this region. Additional data being collected in and around cities as part of AMMA will help to improve current estimates. There are also important sources of NO_x from lightning and soils. Both these sources are very uncertain. It has already been suggested that soil emissions over West Africa are a factor of 2 higher than previously thought (Jaeglé et al., 2004). Biogenic emissions of VOCs are also significant over West Africa and can result in the production of secondary organic aerosols over the region. Mineral dust is a significant contributor to the high aerosol optical depths seen over the Sahara/savannah regions and in air masses transported out of the region (e.g. over the North Atlantic). Understanding about interactions

between aerosols and trace gases still requires further investigation (and will take place as part of WP2.4 and 4.1.3 later in the project). At present, global models within the AMMA-EU project have been run as either chemistry or aerosol models.

Here, results are presented from participating models showing comparisons with data collected in during the period 2000 to 2003 (identified in WP4.3 as evaluation years in the AMMA project). The years 2000 and 2003 were chosen as specific years for comparison of climate and chemistry-aerosol models. Prior to the collection of new data during the SOPs, several, rather limited, chemical datasets are available which can be used to evaluate model performance. Comparison with satellite tropospheric column data from GOME (NO_2) and MOPITT (CO) during this timeframe can provide information on the accuracy of emission inventories being used in the models, and in particular, biomass burning emissions. Analyis and comparison with MODIS or AERONET aerosol optical depths gives an insight into the magnitude of the mineral dust source over West Africa, and the contribution from other aerosol sources such as black carbon and organic aerosols. Transport processes, such as boundary layer exchange and deep convection, clearly influence the vertical redistributions of trace gases and aerosols over West Africa, especially in the wet season. Therefore, it is very useful to compare model results to vertical profile data collected by MOZAIC aircraft during 2002 and 2003 during take-off and landing at various West African cities. This kind of analysis will be repeated using the SOP data when vertical profiles of many more species will be measured up to an altitude of 19km allowing a much more comprehensive evaluation of model performance. Finally, surface data collected as part of the IDAF network allows evaluation of seasonal cycles of surface concentrations (e.g. NO_2, BC) and wet deposition of species such as nitrate ($NO3^-$) produced primarily from washout of nitric acid and nitrate aerosol.

2. The Models

The global models whose results are discussed are the following:

(i) **MOCAGE** (CNRM/ CNRS-LA – Peuch, Josse, Peuch) - the MOCAGE (Modèle de Chimie Atmosphérique à Grande Echelle) model was run at 2 x 2 degree resolution globally with 47 vertical levels extending from the surface up to 5 hPa. It was run for 9 months for the year 2000 forced with Météo-France ARPEGE operational analyses every 6h. The model runs with a semi-Lagrangian advection scheme based on Williamson and Rasch. The chemistry scheme is based on on the RACM chemical scheme of Stockwell et al. in the troposphere and the model REPROBUS (Lefèvre et al.) in the stratosphere. The performance of the advection, turbulence/convection and wet scavenging representation are discussed in (Josse et al., 2004a, Josse, 2004b). Concerning dry deposition of species, MOCAGE uses a detailed scheme including a refined treatment of the stomatal resistance term from the land surface scheme of Météo-France (e.g. Michou et al., 2005a). For the present simulations, global anthropogenic emissions were specified using the (Dentener et al., 2006) prepared for the fourth IPCC assessment. Emissions are provided for the year 2000, with 1° spatial resolution and monthly values. Biomass burning emissions are discussed in the next section.

(ii) **LMDz-INCA** (CNRS-SA/IPSL – Pham, Bouarar, Law, Filiberti, Hauglustaine) - LMDz4-INCA couples the Laboratoire de Météorologie Dynamique general circulation model (LMDz) – version 4, and the Interaction with Chemistry and

Aerosols (INCA) module [Hauglustaine et al., 2004]. Simulations were performed at a resolution of 96 longitudes x 72 latitudes (corresponding to 2.5 x 3.75 degrees) and 19 levels. The model includes detailed VOC chemistry and the monthly emissions for gaseous species used in LMDz4-INCA are as follows - anthropogenic emission inventory based on EDGAR V3.0 (Olivier et al., 2001); biomass burning emissions based on the inventory of Van der Werf et al. (2003) averaged over the period 1997-2001; biogenic emissions (isoprene, terpenes, acetone and methanol); NO soil emissions based on the parameterization of Yienger and Levy (1995). Lightning NO_x emissions parameterized according to Price and Rind (1992).

(iii) **TM4** (KNMI – van Noije, Meijer, Velthoven) is a three-dimensional chemical transport coupled off-line to ECMWF meteorological fields . The model includes NMHC chemistry and sulphur aerosols. Emissions of NO_x, CO, NMHC, SO_2 and NH3 are specified on a 1°x1° grid and taken from the RETRO emissions inventory. The model was run at a horizontal resolution of 3 x 2 degrees. A detailed description of the model is given in Van Noije et al. (2006) and references therein.

(iv) **ORISAM-TM4** (CNRS-LA - Liousse, Guillaume, Junker) - two versions of the TM4 global model (developed at KNMI) have been used run at 3 x 2 degree resolution with 9 vertical levels. A tracer version was run to test emission inventories of black carbon and primary organic carbon. In addition, a full chemistry-aerosol version was run, called ORISAM-TM4, which takes into account secondary organic and inorganic formation of aerosols from gaseous precursors onto primary particles including considerations of microphysical aging (8 classes of diameter (bins) scheme with nucleation, coagulation and condensation processes). In these preliminary simulations, the organic precursors were toluene, xylene and long-chain alkanes and alkenes for the anthropogenic components and terpenes for the biogenic components.

3. Ozone Distributions over West Africa

Ozone distributions over West Africa are dependent on emissions of precursors, photochemical processes producing and destroying O_3, transport processes and dry deposition on different surfaces. Photochemical production of O_3 depends primarily on NO_x levels as well as VOC and CO levels whereas photochemical destruction depends on levels of HO_x radicals (OH, HO_2) and water vapour. The hydroxyl radical (OH), which itself is produced by O_3 photolysis and subsequent reaction with water vapour, is important for the oxidising capacity of the troposphere since it is the primary oxidant of many VOCs, CO and CH_4. It is also important to understand the balance between short-lived species such as NO_x and HO_x (chemical lifetimes of seconds to hours) and longer-lived reservoir species such as nitric acid (HNO_3), peroxy-acetyl nitrate (formed from reaction of NO_2 and VOC degradation products), formaldehyde (HCHO) and hydrogen peroxide (H_2O_2). Several of these species are soluble and so, washout in deep convective clouds can lead to loss of nitrogen or hydrogen containing substances from the atmosphere thereby influencing the oxidising capacity and the potenial to produce O_3. Dry deposition of gases which varies with surface type (vegetation, soil, water) is also an important loss process for O_3. Here, the ability of current state-of-the-art chemistry models, is evaluated by comparing to monthly variations seen in observations of O_3 and its

precursors (NO_2 and CO). These are currently the only observations available. During the SOPs many other species will be measured (e.g. HNO_3, PAN, OH, RO_2, HCHO, NO, VOCs).

a) Carbon monoxide budget

The MOCAGE model has been used to investigate the contribution of transport to the CO distribution over West Africa. Biomass burning emissions correspond to the more recent GFED dataset averaged over 1997 to 2002 (Van der Werf et al.,2006). Although, a finer vertical profile is provided in the GFED dataset, the emissions were grouped into 3 altitude bins in MOCAGE (0-1km, 1-2km and 2-3km). By way of illustration, Figure 1 shows the total emissions of CO, NO_x and CH_4 used in MOCAGE at the surface (corresponding to the 0-1km component) and at 2500m (corresponding to the 2-3km) for the month of January 2000. Over the AMMA domain, the dominant source for the three species is indeed biomass burning. The hotspots for all the species correspond to fire locations, with different patterns in the PBL and in the free troposphere. Only the fires between 5° and 10°N and East of 10°W are strong emitters above 2km (in this emission inventory), whilst the continental band between 5° and 10°N emits into the PBL in this dataset.

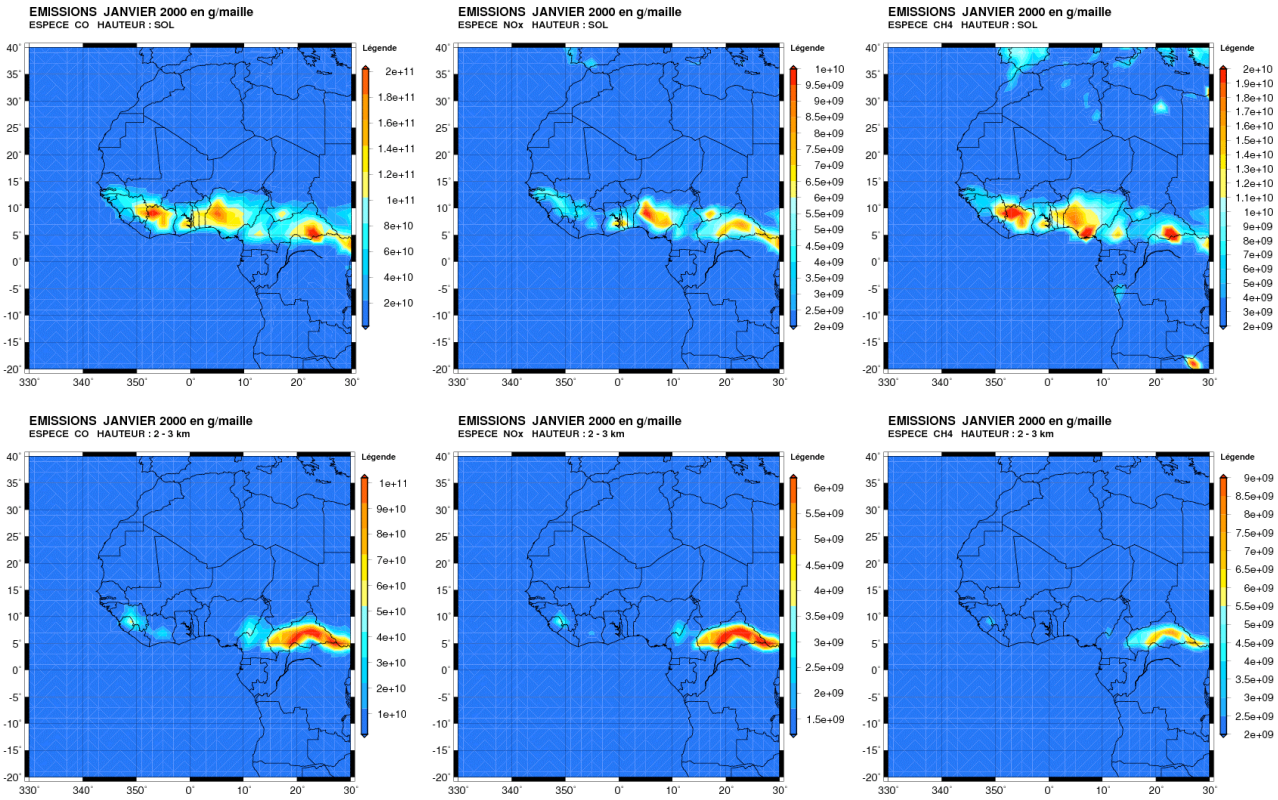

Figure 1. Surface and altitude (2-3km) emissions of CO (left), NO_x (middle) and CH_4 (right) in the MOCAGE model for January 2000 in g per 2°x2° grid-cell.

This biomass burning emission inventory appears to be consistent with the actual fire counts deduced from ATSR-2 on board ERS-2 for the month of January 2000 even though the emissions are actually average January emissions from 1997 and 2002 (see Figure 2). The fire pixel density is higher where altitude emissions are stronger, corresponding to the zones where the fires extend over a greater area.

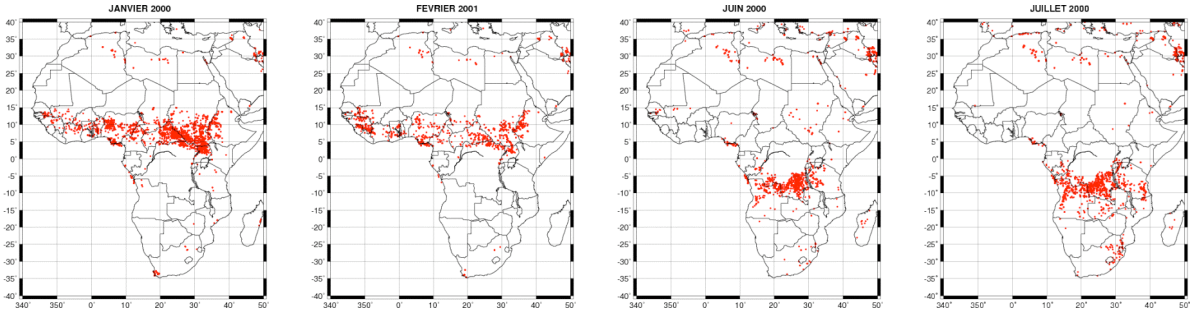

Figure 2. Fire pixels in January, February, June and July 2000 (from left to right) as seen by ERS2/ATSR-2. ATSR world fire atlas: http://dup.esrin.esa.it/ionia/wfa/index.asp.

Figure 3 shows the emissions in the PBL (0-1km) for the same 3 trace gases, but for July 2000. Again, the comparison with fire pixels of Figure 2 is satisfactory. Therefore, it appears that the distribution of emissions in the Van der Werf (2006) dataset is good in terms of hotspots localization and of seasonal variability but the actual magnitude is still very uncertain. Efforts on emissions within AMMA will help better characterise the emission factors for the different ecosystems over West Africa (see also aerosol section).

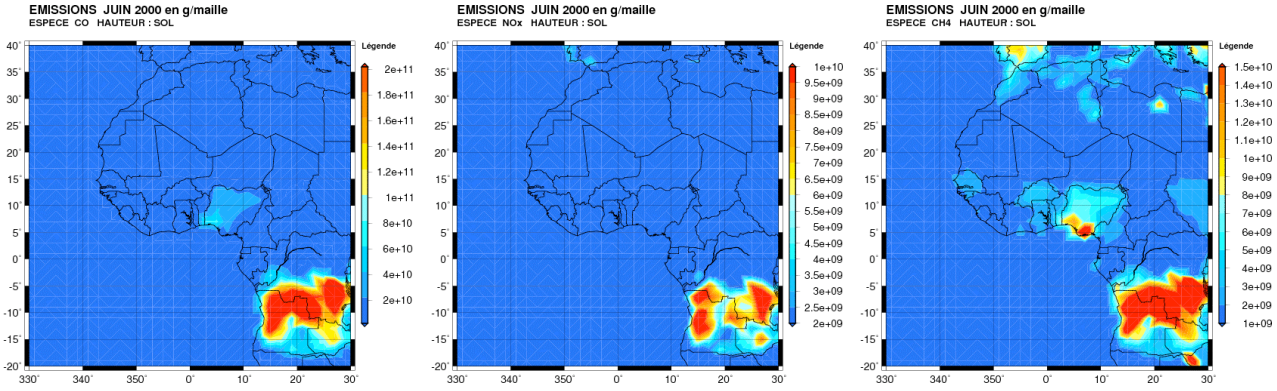

Figure 3. Surface emissions of CO (left), nitrogen oxides (middle) and methane (right) taken into account for the month of June 2000 in the MOCAGE model. Emissions are given in g per 2°x2° grid-cell.

Comparison and assimilation of MOPITT CO data

The MOCAGE model has also been compared with CO data from the MOPITT instrument which can provide information on CO distributions in the lower, mid and upper troposphere. Results for the months of February and July 2001 are shown in Figs. 4 and 5, respectively. It can be seen that, in general the model captures the spatial distribution of CO quite well at the different levels. However, in February there is a tendency to overestimate concentrations in burning regions in the lowest layer and underestimate in the mid-troposphere. This may point to problems with exchange between the PBL and the free troposphere. During the summer months, the CO distribution is dominated by burning in central Africa. Here, MOCAGE appears to transport too much CO into the upper troposphere. It will be interesting to quantify the amount of CO from burning regions transported into the ITCZ region over West Africa at this time of year and to compare this with local sources such as CO production from degradation of biogenic VOCs emitted by forests.

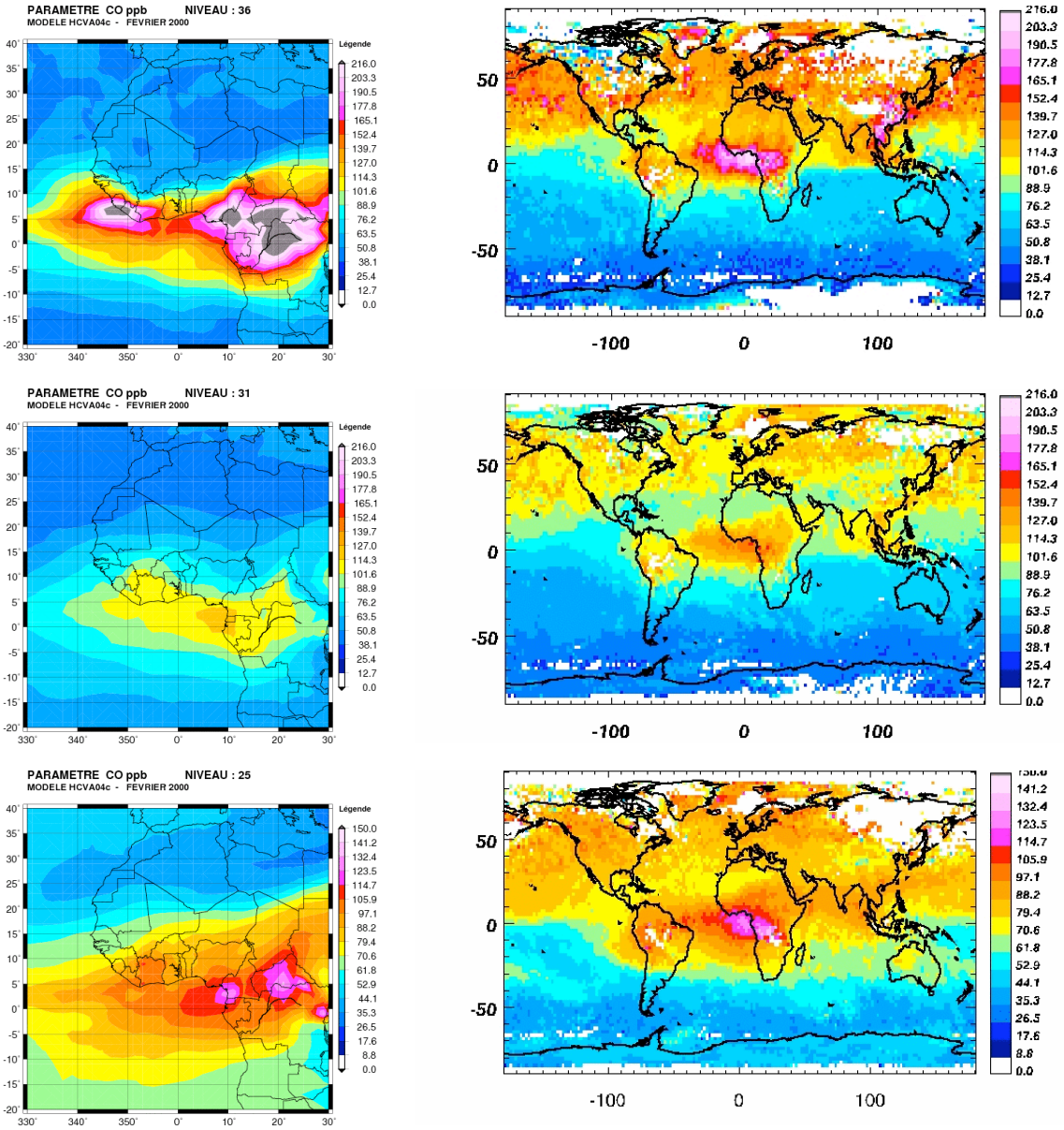

Figure 4. 700hPa (top), 500 hPa (middle) and 250 hPa (bottom) carbon monoxide mixing ratios (ppb) for February 2000 in MOCAGE simulations (left) and for February 2001 in MOPITT retrievals (right).

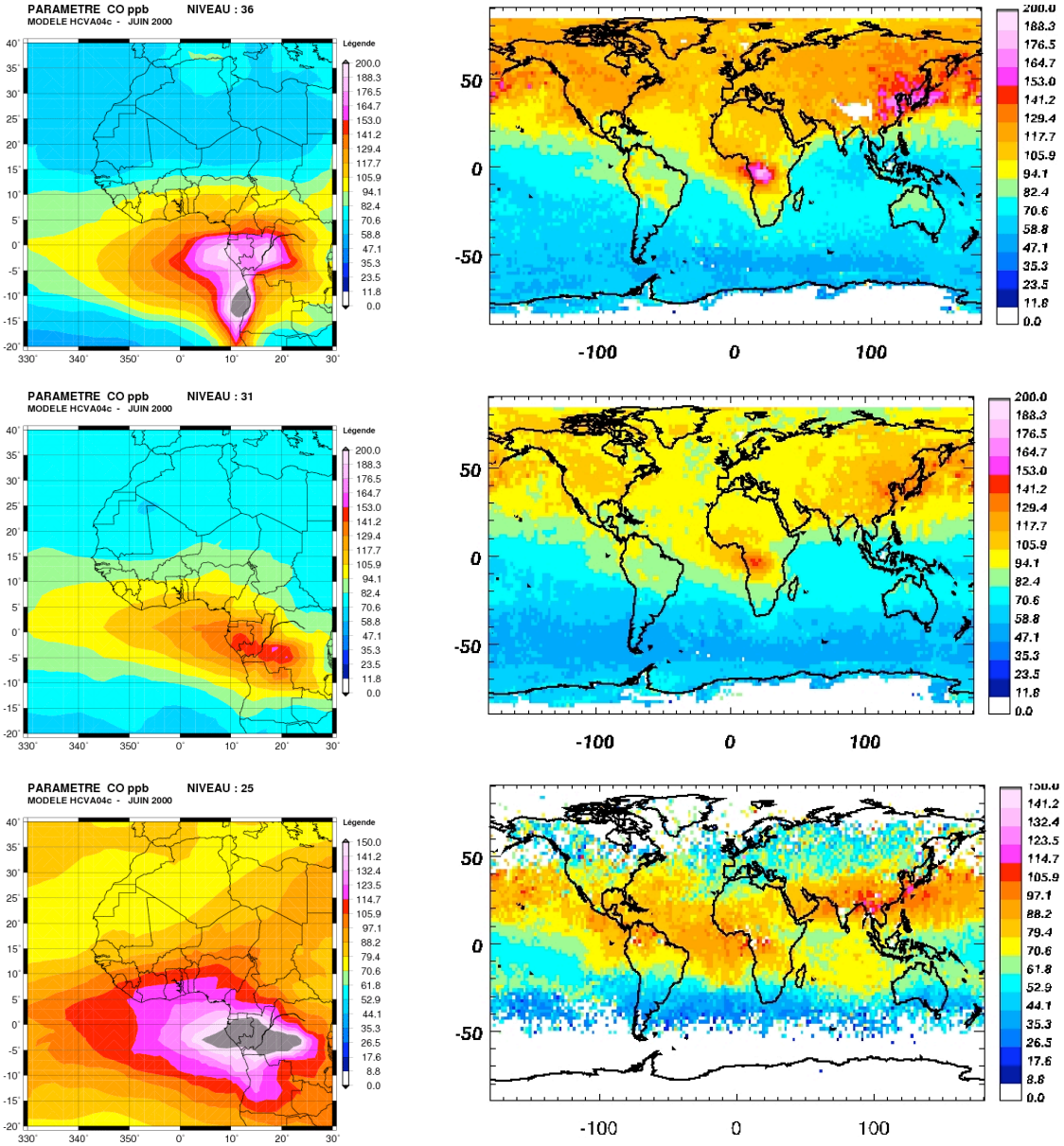

Figure 5. 700hPa (top), 500 hPa (middle) and 250 hPa (bottom) carbon monoxide mixing ratios (ppb) in MOCAGE simulations (left) and in MOPITT retrievals (right) for June 2000.

CO vertical profiles from MOPITT have also been assimilated into MOCAGE using a sequential assimilation technique based on a suboptimal Kalman filter. This kind of analysis can provide information on the magnitude of emissions used in models and also the vertical redistribution of emissions as the sensitivity of the data from the satellite varies with altitude. When, MOPITT data was assimilated into MOCAGE for a 2-month period in spring 2001, the overestimation of CO in high emissions areas over West Africa is considerably reduced (see Figure 6).

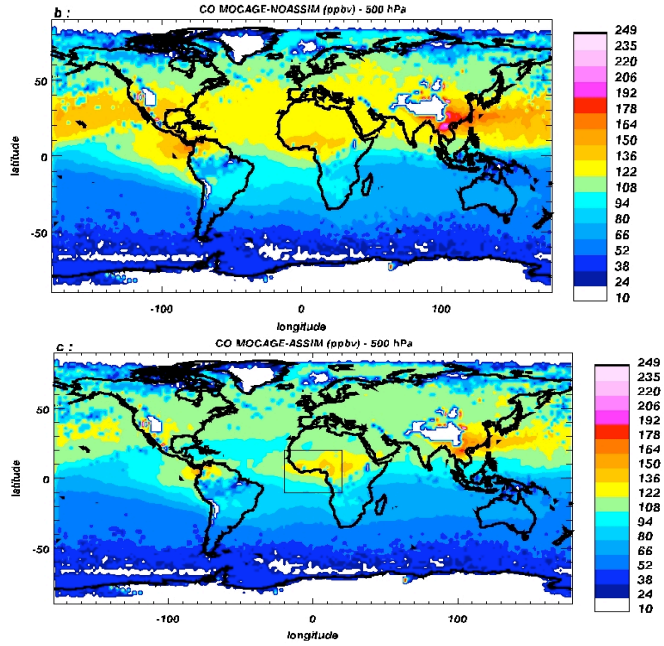

Figure 6. Global mean CO (ppbv) calculated by MOCAGE during the period between March 1 and May 6, 2001. Top: without assimilation, bottom: with assimilation of MOPITT CO

CO budget over West Africa

MOCAGE results with assimilated CO were analysed for a period of three successive 15 day periods in terms of average distributions over West Africa and contributions to the CO budget from transport and chemical sources. It was found that the horizontal and vertical CO distributions are strongly dependent on the characteristics of the large scale flows during spring, marked by the onset of the low level southerly monsoon flow and the gradual increase of the well known African and tropical easterly jets at middle and upper levels, respectively. The total transport by the mean flow (horizontal plus vertical advection) is important for the CO budget since it mostly compensates the local sink or source generated by chemical reactions (loss with OH or production from VOC oxidation) and small scales processes. The major source of CO, concentrated in the lower troposphere (1000-800 hPa), is mainly due to convergent low level flow advecting CO from surrounding regions and surface emissions (biomass burning). Vertical transport removes 70% of this low level CO and redistributes it in the middle troposphere (800-400hPa) where chemical reactions and horizontal advection contribute, in nearly equal proportions, to the removal of CO over this region. A smaller proportion is transported upwards into upper troposphere, then horizontally out of the domain. Figure 7 shows profiles of the sources/sinks due to total transport and small scales processes. The CO mean tendency during MA2, AP1 and AP2 is negative below 500 hPa (not shown). However it is more than an order of magnitude smaller than the different terms that contribute to the CO budget: *advective processes*, *local sources/sink*. Hence, at each level, the different CO production/loss terms balance each other quite well. Strongest contributions are in the lower (>600 hPa) troposphere: maximum sources and sinks occur between the surface and 800 hPa. At the lowest levels (>950 hPa), sources originate from surface emission and turbulent diffusion whereas advection and OH reaction act as a sink. At levels near 800 hPa, source and sink origins change: large scale advection supplies this layer with CO while subgrid vertical transport (deep convection) processes generate an upward transport (the 900-700 hPa layer feeds the 700-80 hPa one with CO), while the destruction with OH represents one third to half of the sink.

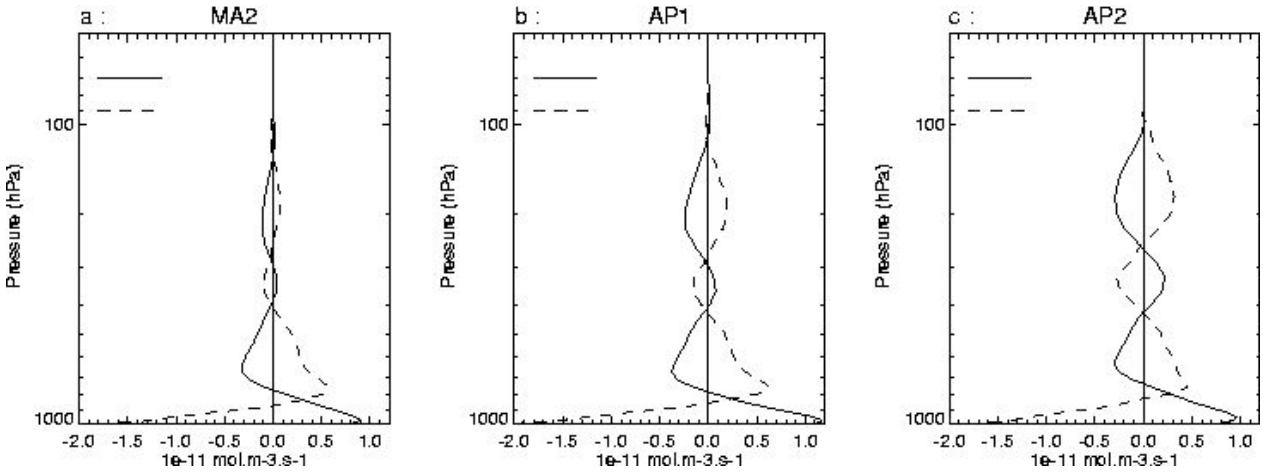

Figure 7. Mean budget of CO over West African domain (see Figure 3) simulated by MOCAGE with assimilation of MOPITT CO for the three periods (a) MA2, (b) AP1, and (c) AP2. The solid, dashed lines correspond to total flux convergence and CO source/sink due to sub-grid scale processes, respectively.

In conclusion, analysis of CO distribution and transport over West Africa during March and April 2001 shows that dry convection resulting from the confluence between monsoon and Harmattan winds is responsible for the CO upward motion as high as 500 hPa. Quantitative study of CO budget reveals a balance between total resolved-scale and sub-grid scale transport, as well as chemical contribution, which are the main source/sink of CO. It will be interesting to apply this kind of analysis to other times of year.

Vertical distributions

In-situ CO and O_3 (see section 3c) data recorded by the MOZAIC (Measurement of Ozone and Water Vapour by Airbus Service Aircraft) programme during 2002 and 2003 have been used to evaluate the vertical distributions of these trace gases in various models. The MOZAIC programme started in 1993 making measurements of ozone and water vapour in the atmosphere using commercial long rang airlines (Marenco et al., 1998) and since 2002 making measurements of CO and NOy in addition. The MOCAGE, LMDz-INCA and KNMI models have been compared to MOZAIC CO profiles collected during landing and takeoff over various cities in West Africa. Figures 8, 9 and 10 show comparisons between the models and MOZAIC over Lagos (6.6N-3.333E) - the most well documented city - in January, February, July and August. The MOZAIC data are averaged over 2002 and 2003 in the MOCAGE figure; LMDz-INCA was nudged with meteorological analyses for the year 2002 and so data for 2002 and 2003 are shown separately; TM4 was forced with ECMWF analyses. Note that often not many profiles are available. For example in January 2002 12 profiles are available over Lagos whereas in June 2002 no data were recorded with only 4 profiles in June 2003.

Results show different behaviours for different models. Note that in the dry season Lagos is likely to be influenced by biomass burning emissions transport from fire regions as well as local anthropogenic emissions. In this season, the models have a tendency to underestimate CO concentrations in the lower troposphere even when a fraction of biomass burning emissions are emitted up to 3km altitude (MOCAGE, TM4). The underestimation at the lowest levels is most probably due to underestimation of local anthropogenic sources. All the models also underestimate concentrations in the layers just above the boundary layer. In LMDz-INCA this may be due to the winds in the model which are too zonal at this time of

year and transport emissions from the main burning areas (to the east) further north in the model. It could also be due to deficiencies in the PBL exchange schemes used in the models.

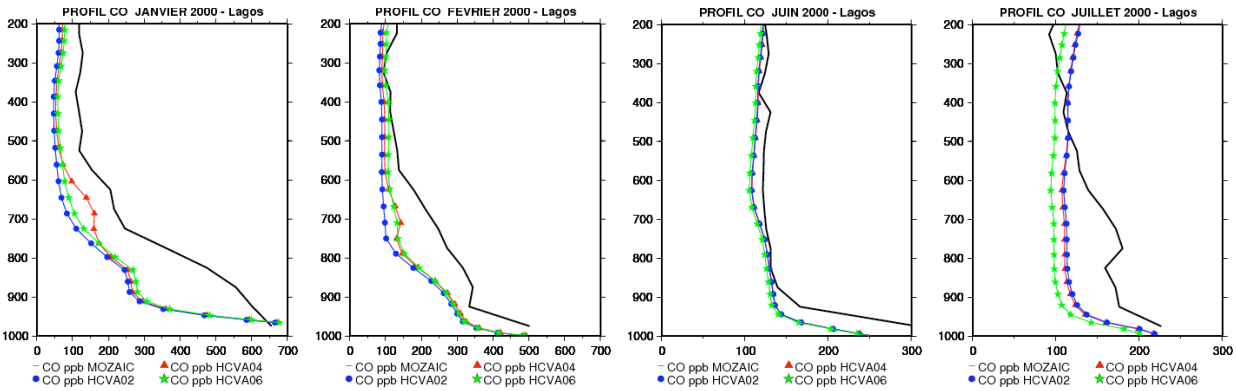

Figure 8. Mean vertical profiles of carbon monoxide for January, February, June and July 2000 (from left to right) in MOZAIC observations (black) over Lagos. Corresponding MOCAGE simulations with altitude emissions taken into account (red), without altitude emissions (blue) and with altitude emissions taken into account but at the surface (green).

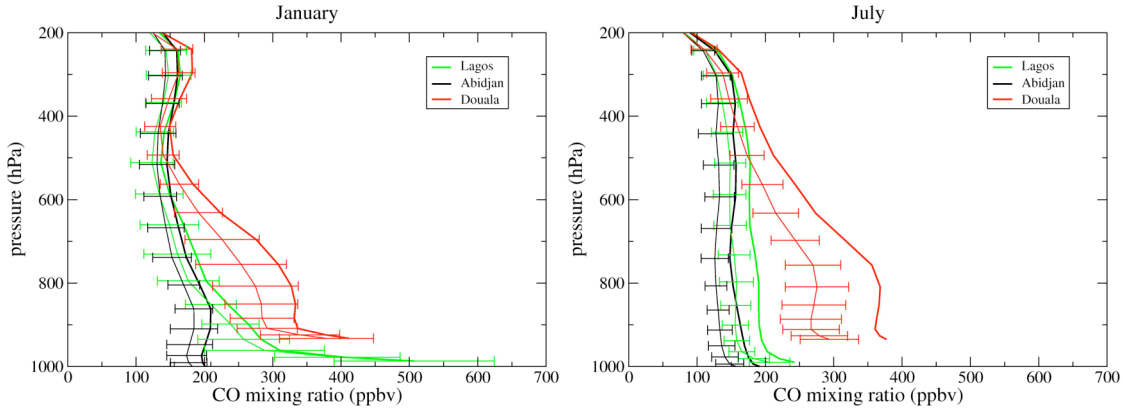

Figure 9. TM4 modelled CO vertical profiles for January and July for Lagos, Abidjan, Douala, based on simulations for the year 2000 using the RETROv1 emissions. The results for surface emissions (thin) are compared with the results obtained by applying an emission height distribution.

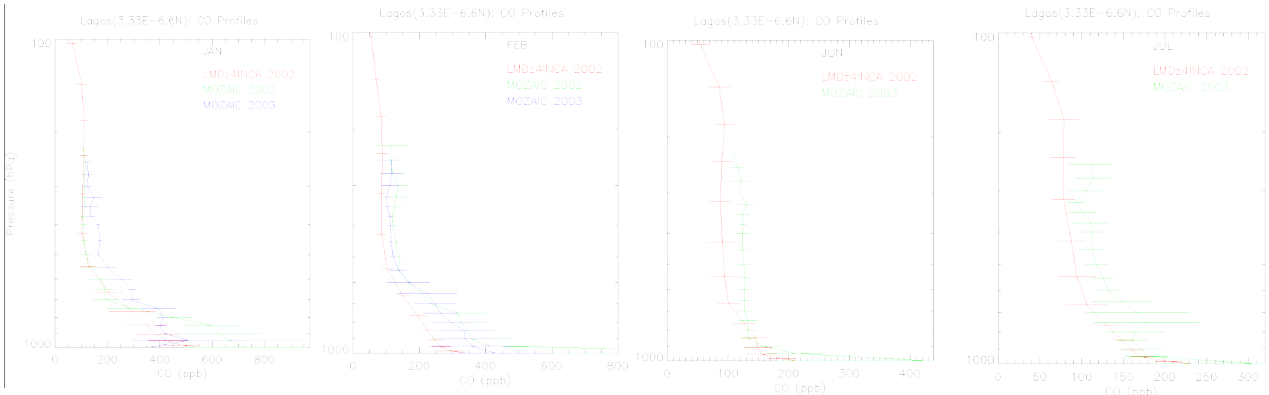

Figure 10. LMDz-INCA modelled CO vertical profiles for January, February, June and July 2002 over Lagos; MOZAIC data shown for 2002 and 2003.

b) Nitrogen budget

Comparison with GOME NO_2 data

The TM4 model has been compared with tropospheric nitrogen dioxide (NO_2) columns from Global Ozone Monitoring Experiment (GOME) for the year 2000. For the interpretation of the differences between modeled and retrieved columns it is important to realize that there are systematic differences among the current state-of-the-art retrievals. Over the biomass burning regions of Africa the BIRA/KNMI retrieval generally gives higher values than retrievals made by the University of Bremen and Dalhousie University. The amounts retrieved by BIRA/KNMI over West Africa and Northern Central Africa can be up to a factor of 2 higher on a monthly basis than the values retrieved by the University of Bremen; over Southern Central Africa the spread among the retrievals is somewhat smaller than this [van Noije et al., 2006]. These differences can be due to the way aerosols and clouds are treated in the retrievals.

The satellite retrieval used in this study is the one produced by the KNMI based on slant-column data from BIRA/IASB. The annual mean NO_2 column density observed over Africa in this retrieval is shown in the top panel of Figure 11. The annual mean is here taken as the mean over all observations made during the year. In order to systematically compare the model with the retrievals, model results were output at 10:30am local time, i.e. close to the overpass time of the ERS-2 satellite, and sampled the data at the times and locations of the observed scenes. This effectively removes the differences related to measurement biases due to incomplete coverage of the satellite observations (van Noije et al., 2006). One of the major uncertainties in our understanding of the chemical composition over West Africa is related to uncertainties in the emissions from biomass burning. For this reason simulations were performed using two recent emission inventories. The first is the Global Fire Emissions Database version 1 (GFEDv1) (van der Werf et al., 2003) and the second is a preliminary version of the wildfire emission inventory prepared within the EU-project RETRO (RETROv1) (Schultz et al., 2006). In both cases the NO_x emissions are estimated based on the emission factors of Andreae and Merlet (2001) taking into account some more recent revisions, especially for savanna burning (M. Andreae, personal communication, 2004). A more detailed description of the model setup of these simulations is given by van Noije et al. [2006] and on www.retro.enes.org, respectively. The GFEDv1 emission estimates generally produce higher NO_2 columns than the RETROv1 emissions over the polluted regions of West and Central Africa, in closer agreement with the BIRA/KNMI retrievals. In both inventories the spatial distribution agrees reasonably well with the observed pattern.

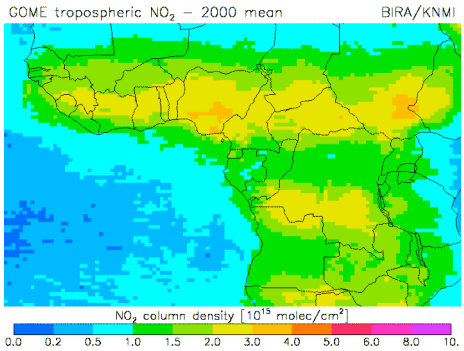

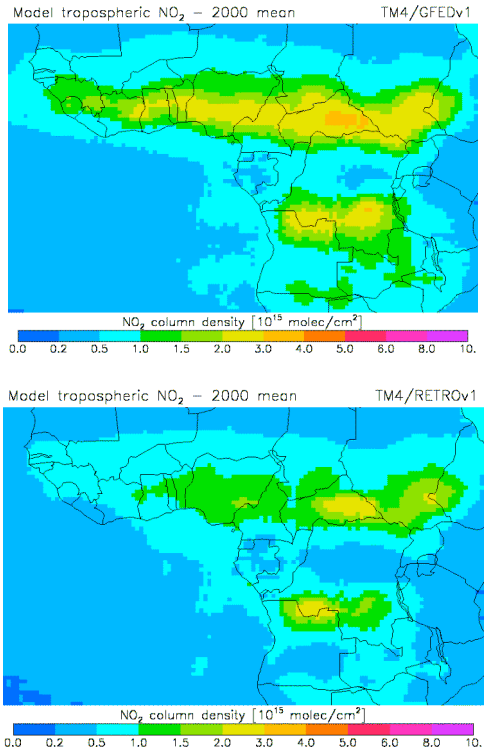

Figure 11. Annual mean tropospheric NO_2 column densities for the year 2000 from the BIRA/KNMI retrieval compared to TM4 model results based on the GFEDv1 and RETROv1 biomass burning emission inventories.

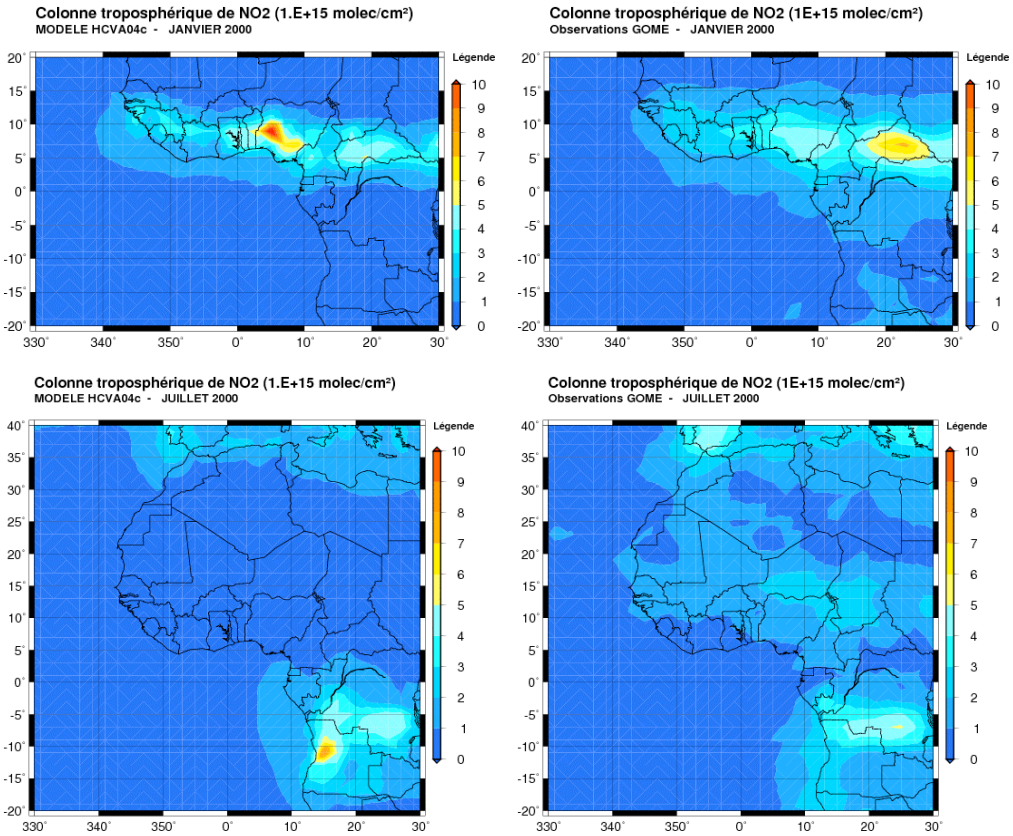

Figure 12. Mean Nitrogen Dioxide tropospheric column simulated by MOCAGE (left) and seen by GOME (http://www.temis.nl, right) for the month of January 2000 (top) and July 2000 (bottom).

It should be noted that the RETRO emissions are currently being revised leading to higher emissions from tropical forest burning (M. Schultz, personal communication, 2006). The GFED group has also improved their inventory in several respects and has just published a new version (GFEDv2) (van der Werf et al., 2006). The MOCAGE model has been run with the more recent Van der Werf emissions including some vertical re-distribution (see CO budget section), but it also tends to underestimate NO_2 columns over West Africa from KNMI/BIRA although results might agree better with lower U. Bremen retrievals. In this case, it can be seen that the model underestimates the columns in the wet and dry season.

For a more quantitative analysis, the TM4 results were also analysed over the domain shown in Figure 11divided into equal-sized quadrants over West Africa (20^oW – 10^oE x 0^oN – 20^oN), northern Central Africa (10^oE – 40^oE x 0^oN – 20^oN), southern Central Africa (10^oE – 40^oE x 20^oS – 0^oN), and a region over the Atlantic (20^oW – 10^oE x 20^oS – 0^oN). For the continental regions of West Africa and northern/southern Central Africa spatial correlations between the annual mean modelled and retrieved NO_2 patterns were calculated. To optimize the comparison, the retrieved pattern was first smoothed to the resolution of the model, i.e. 3^o longitude x 2^o latitude. The resulting scatter plots are shown in Figure 13 with the corresponding spatial correlation coefficients given in Table 1. The spatial correlations between the modelled and retrieved patterns are highest over West Africa and northern Central Africa, where the two inventories give comparable results. Over southern Central Africa the correlation is somewhat lower, especially when using the RETROv1 emissions.

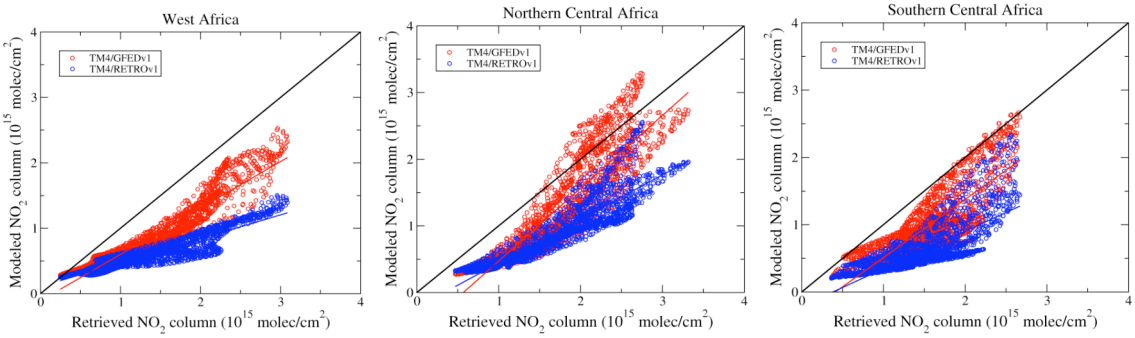

Figure 13. Scatter plots of the TM4 modelled versus retrieved NO_2 column densities over the regions of West Africa and northern and southern Central Africa for the simulations based on the GFEDv1 and RETROv1 emission inventories, respectively.

Region	Spatial correlation	Temporal correlation
West Africa	0.947 (0.931)	0.784 (0.604)
Northern Central Africa	0.904 (0.910)	0.931 (0.906)
Southern Central Africa	0.843 (0.754)	0.910 (0.784)

Table 1. Spatial and temporal correlations between modelled and retrieved NO_2 columns over the regions of West Africa and Northern and Southern Central Africa for the year 2000. Correlations coefficients apply to the TM4 model with GFEDv1 (RETROv1) biomass burning emissions compared to the BIRA/KNMI retrieval. Spatial correlations are derived on the basis of the annual mean patterns; temporal correlations on the basis of the regional monthly means.

The seasonal cycles in tropospheric NO_2 over West Africa, northern Central Africa, and southern Central Africa are shown in Figure 14. During the wet season when the fire activity is low, the TM4 model systematically underestimates observed NO_2 columns. This is probably due to an underestimation in NO_x emissions from soils. In the model these are based on the parameterization of Yienger and Levy (1995) constrained to a global total of 6.0 Tg

N/yr. Jaeglé et al. (2004) presented evidence of strongly enhanced NO_x emissions from soils over the Sahel during the rainy season, also based on analysis of GOME data. New improved emission estimates for soil NO_x will be produced in WP2.4 and should be incorporated into the global models (Serca et al. – CNRS-LA). An indication of the contribution from biomass burning is found by comparing the NO_2 columns during the dry season compared to the wet season. Bearing in mind the uncertainties associated with the retrieval and modelling of tropospheric NO_2 columns (van Noije et al., 2006), these results indicate that the seasonal cycles produced using the GFEDv1 emissions are of the correct order of magnitude, while the RETROv1 inventory is underestimates the emissions from this source. The temporal correlations coefficients corresponding to the seasonal cycles of Figure 13 are also included in Table 1. Using the GFEDv1 emissions, we find temporal correlations higher than 0.9 over northern and southern Central Africa and values lower than 0.8 over West Africa. Using the RETROv1 emissions, the temporal correlations are significantly lower, especially over West Africa and southern Central Africa. However, differences between the KNMI/BIRA and U. Bremen retrievals need to be resolved in order to make more quantitative statements about the magnitudes of biomass burning emissions used in global models.

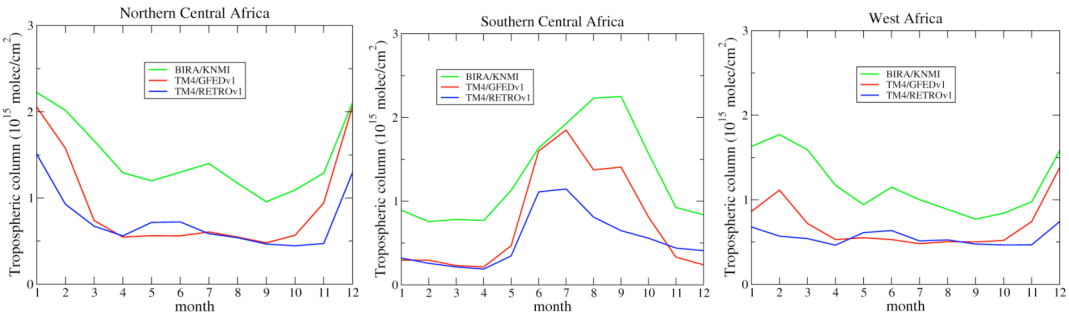

Figure 14. Seasonal cycle in retrieved and TM4 modelled tropospheric NO_2 over northern Central Africa, southern Central Africa and West Africa for the year 2000.

The two TM4 model runs presented above not only use different biomass burning emissions, but also use different meteorological input data. The run using the GFEDv1 emissions is driven by operational data from the European Centre for Medium-Range Weather Forecasts (ECMWF), while the run using the RETROv1 emissions is driven by the ECMWF reanalysis ERA-40. We have checked that the use of ERA-40 instead of operational data only a minor impact on tropospheric NO_2 columns. As an example Figure 15 shows the annual mean column density from a run of the TM4 model using the RETROv1 emissions in combination with operational meteorological data.

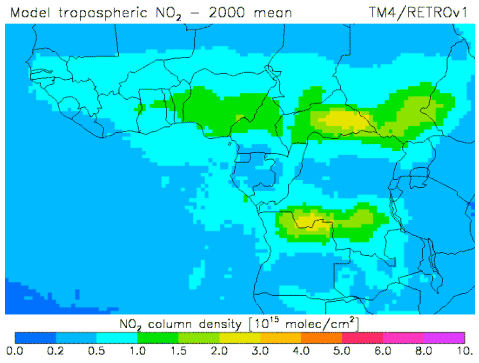

Figure 15. Annual mean tropospheric NO_2 column densities for the year 2000 from a TM4 simulation using the RETROv1 emissions and operational meteorological data.

Comparison with surface IDAF data

Results from the LMDz-INCA model have been compared to surface measurements of NO_2, HNO_3, nitrate wet deposition and precipitation from the IDAF network for period 1994-2002 (see Figure 16). The IDAF (IGAC/DEBITS/Africa: International Global Atmospheric Chemistry/Deposition of Biogeochemically Important Trace Species/Africa) programme started in 1994 with the aim of measuring wet and dry deposition fluxes, and to identify the relative contribution of anthropogenic sources factors regulating these fluxes (e.g. see Yoboue et al., 2005). Specially designed precipitation collectors have been installed at 10 African network stations to produce atmospheric chemical measurements (gaseous, precipitation, aerosol chemical composition) (Galy-Lacaux et al., 1998). In this case, model results from a climatological simulation have been compared to the data (see Figure 16).

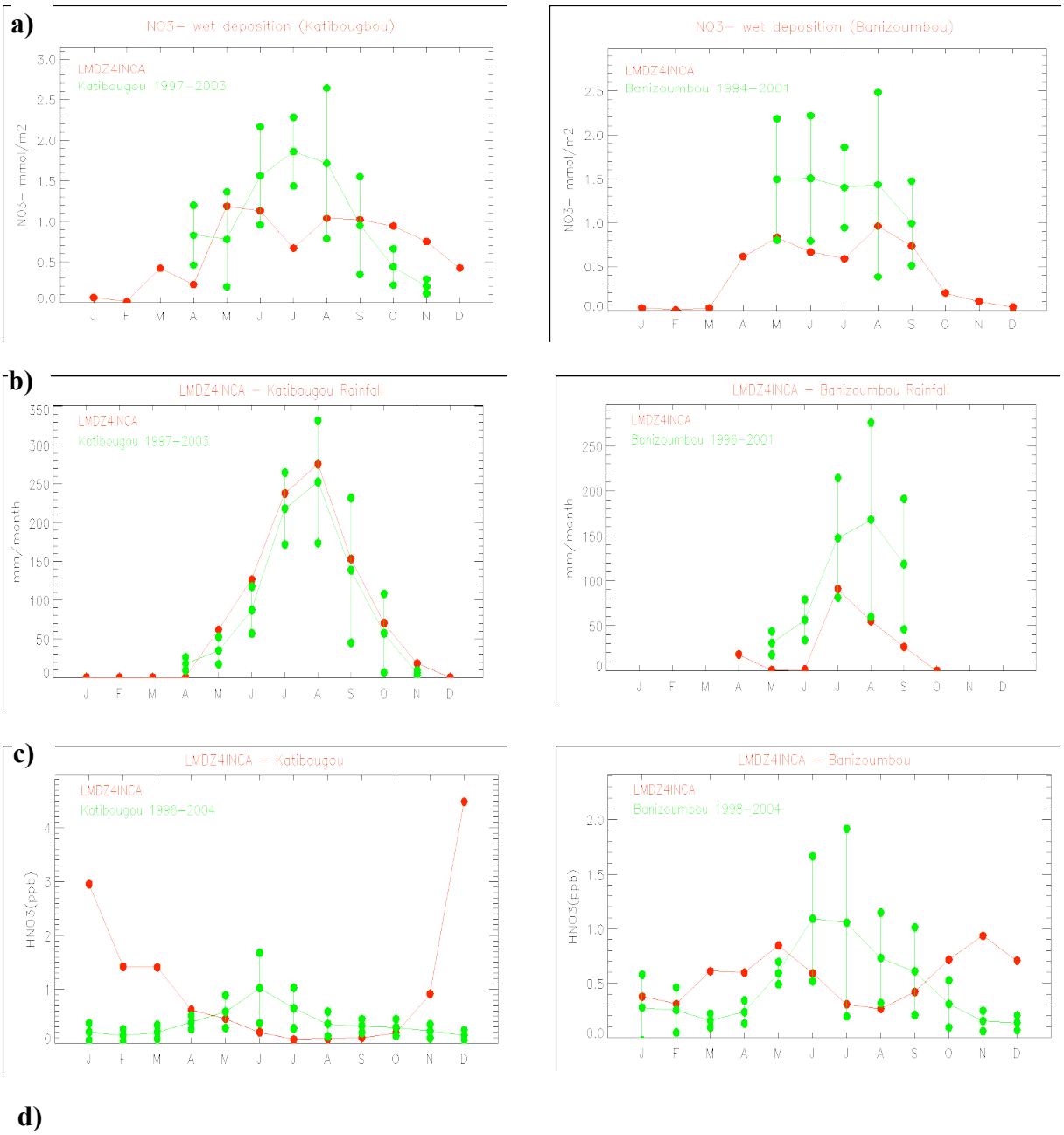

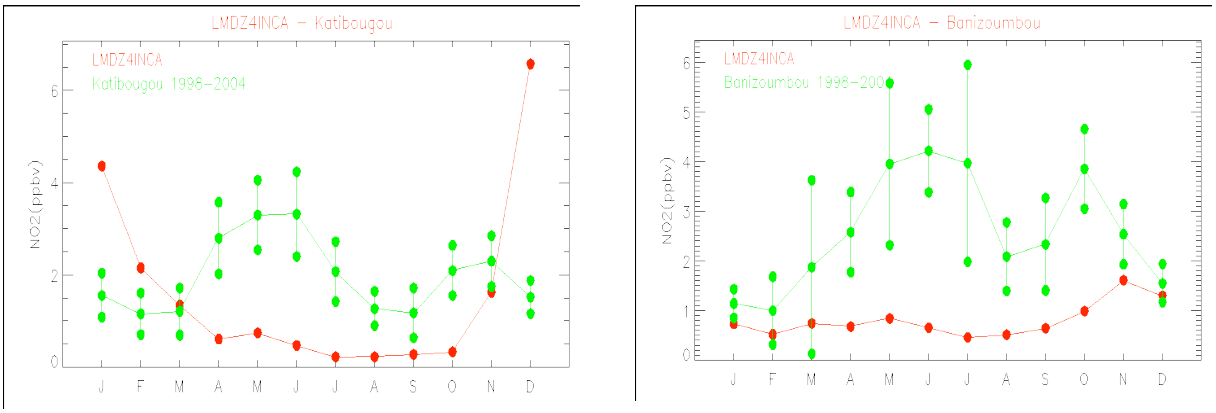

Figure 16. Comparison of LMDz-INCA (red) seasonal variation of nitrate wet deposition (a), precipitation (b), nitric acid (c) and nitrogen dioxide (d) with the IDAF measurements (green) at Katibougou(10.52N-7.33W) and Banizoumbou(13.31N-2.38E) stations.

Results for two IDAF sites, Katibougou (10.52N, 7.33W) and Banizoumbou (13.31N, 2.38E) representative of the Sahelian region, are presented here. Monthly mean chemical rainfall contents at Katibougou and Banizoumbou were computed for the period 1997-2003 and 1996-2001 periods, respectively. Gaseous NO_2 and HNO_3 measured surface concentrations are also computed for seasonal time scale for the full 1998-2004 period (Galy-Lacaux, pers. comm.). The LMDz-INCA model underestimates NO_2 mixing ratios during the wet season (Figure 16d). This is probably due to the fact that current emissions do not take into account the strongly enhanced NO_x emissions from soils over the Sahel as suggested by Jaegle et al. (2004). This leads to an underestimation of HNO_3 from March to September at both sites (Figures 16c). Nitrate levels are also underestimated at this site but it should be remembered that as much as half the contribution to nitrate could be in the from of nitrate aerosol associated with soil or dust emissions. Heterogeneous conversion of HNO_3 on dust could also influence gaseous HNO_3 levels, and subsequent uptake in rainfall. These factors are being studied in greater detail and will make use of results from work on these processes in WP2.4. At Katibougou, on the contrary, modelled NO_x emissions from biomass burning are overestimated in January and December (Figure 16d) which results in too much conversion into HNO_3 compared to observations (Figure 16c). Modelled and observed precipitation (Figure 16b) is in good agreement at Katibougou.

c) Ozone budget

Figure 17 shows a comparison between TOMS column O3 and model results from MOCAGE for the months January and July 2000. The spatial pattern is reasonably well represented in January but values are too high possibly suggesting too much O3 production downwind from biomass burning emission during this season. In the summer period, the model signal is too weak – reasons for this difference are being investigated.

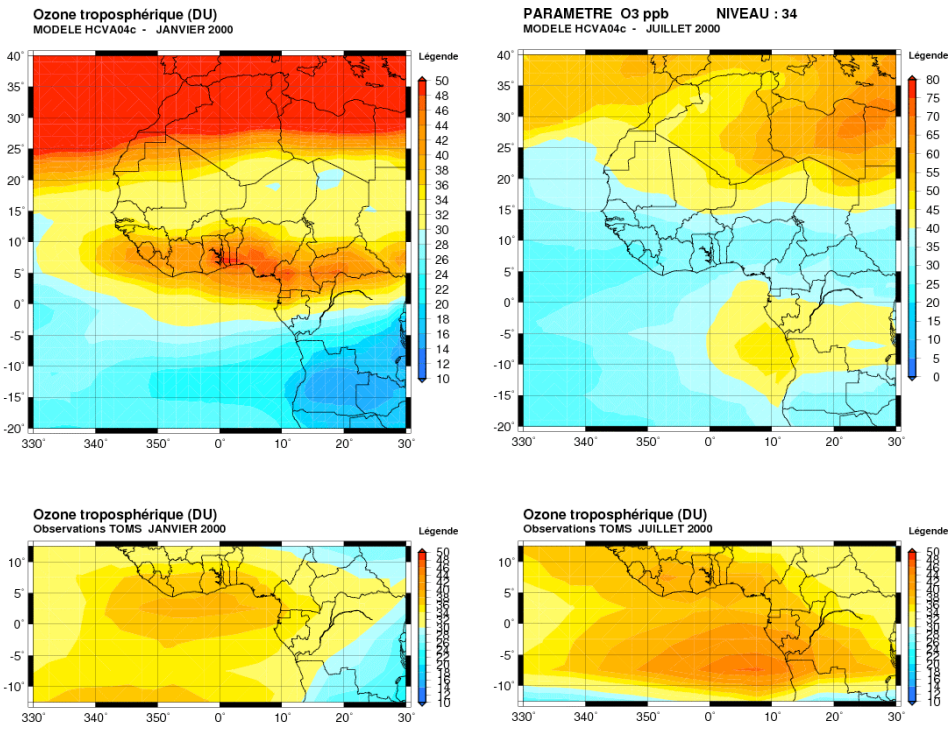

Figure 17. Mean tropospheric ozone column for January 2000 (left) and July 2000 (right) for MOCAGE (top) and CCD/TOMS (bottom).

Vertical O_3 profiles over West Africa

Figure 18, 19 and 20 show comparisons between MOZAIC O3 vertical profiles and the MOCAGE, TM4 and LMDz4-INCA models, again for winter and summer months. During the dry season over the Lagos region, the impact of biomass burning emissions is visible in the measured profiles with an enhancement of O_3 concentrations in the lower troposphere (e.g. Figure 20a) up to 80 ppbv. The LMDz4-INCA reproduces quite well the vertical O_3 distribution. The model tends, however, to overestimate the concentrations below 900 hPa and the maximum measured at 750hPa is simulated at 850hPa. This overestimation could be due too much photochemical production (although CO emissions are underestimated) or due to a vertical mixing problem in the boundary layer. In summer months, LMDz-INCA reproduces reasonably well the vertical O_3 profiles although there are observed peaks in the lower and mid troposphere which are not captured. These are probably related to transport of biomass burning plumes from the Southern Hemisphere over central Africa as discussed by Sauvage et al. (2005). Sauvage et al. (2005) used trajectories from the Meso-NH model to look at this transport related to small-scale convection. The data collected during the AMMA SOP2 as well as ozonesonde data being collected at Cotonou should allow a more thorough investigation of this phenomenon.

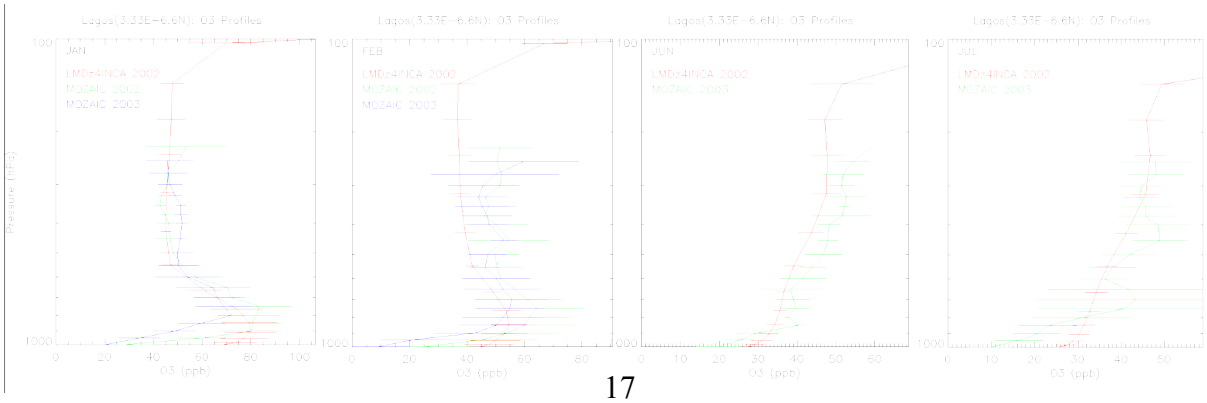

Figure 18. Monthly mean ozone and carbon monoxide vertical profiles in January (a), February (b), June (c) and July (d) modelled by LMDz4INCA (red) and recorded by MOZAIC in 2002 (blue) and 2003 (green) over Lagos (6.6N-3.33E).

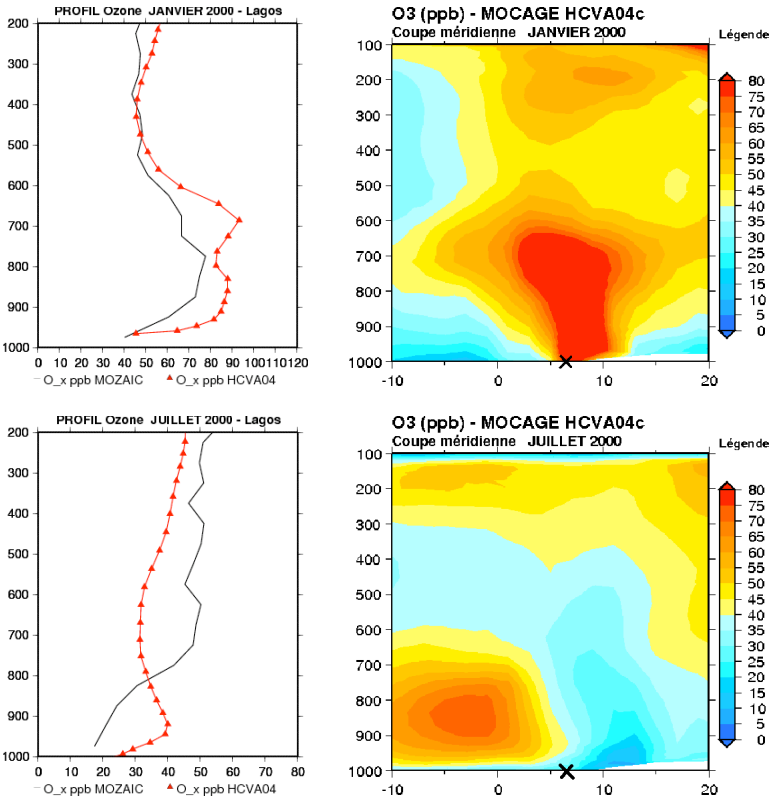

Figure 19. Mean ozone vertical profile over Lagos for MOCAGE and MOZAIC observations (left) and longitude-altitude plot of MOCAGE at the latitude of Lagos for January 2000 (top) and July 2000 (bottom).

For the TM4 simulation using the RETROv1 emissions O_3 vertical profiles for the MOZAIC airports of Lagos (Nigeria), Abidjan (Ivory Coast) and Douala (Cameroon) in the Gulf of Guinea and Brazzaville (Congo) in Central Africa have been analysed. The resulting profiles for the year 2000 are presented in Figure 20. High O_3 levels can be seen in the mid-troposphere which are also seen in the MOZAIC data (not shown) and are linked to biomass burning and local convection over central Africa as noted previously. It can also be seen that the TM4 also fails (like the other models) to capture any long-range transport from this region into the ITCZ region over West Africa.

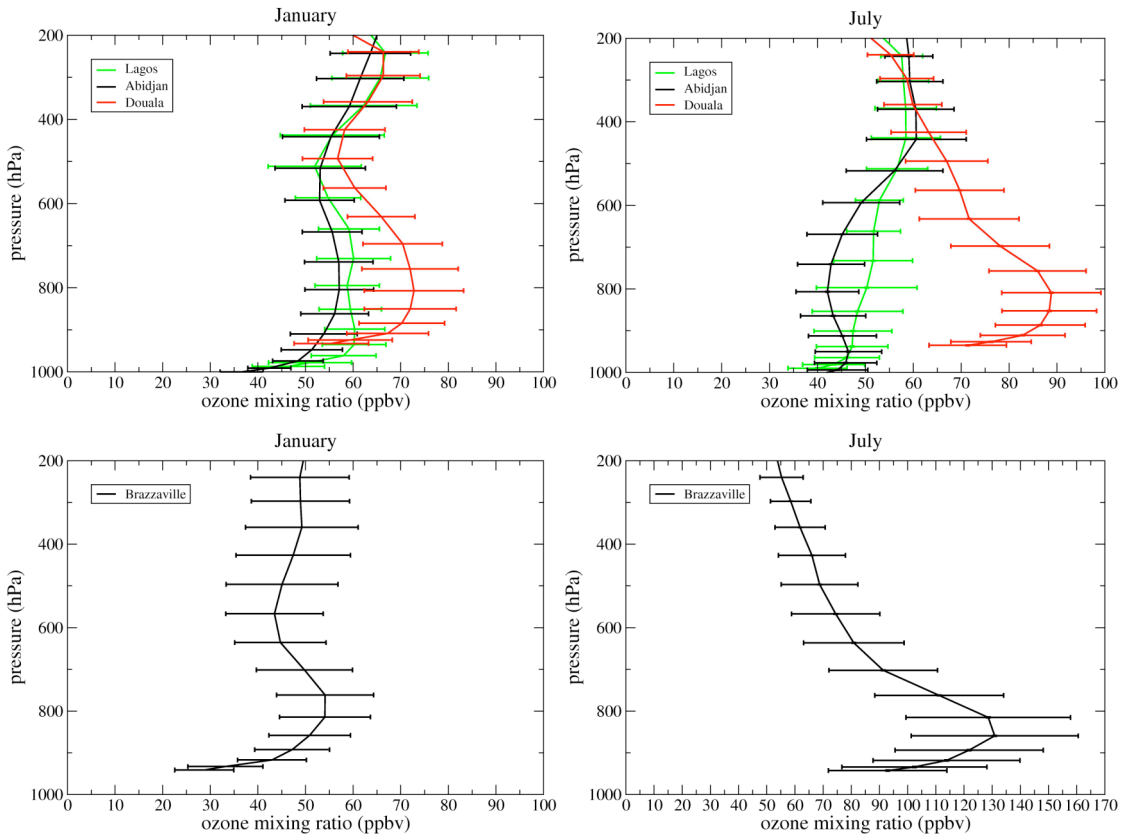

Figure 20. Modelled O_3 vertical profiles for January and July for Lagos, Abidjan, Douala (top) and Brazzaville (bottom), based on a simulation for the year 2000 using the RETROv1 emissions.

In Figure 21 corresponding seasonal cycles in the ozone concentration at 250, 500 and 750 hPa from TM4 are compared with the MOZAIC measurements for the year 2000 over different locations. The corresponding seasonal cycles based on the MOZAIC data for period April 1997–March 2003 are those presented in the paper of Sauvage et al. (2005). For clarity the standard deviation in the modelled monthly means is indicated only for Brazzaville (unconnected error bars). The standard deviations in modelled and observed monthly means are of the same order of magnitude. The simulated monthly means are generally within or close to the range indicated by the measurement, indicating that the model does not have a strong bias in simulated the ozone concentration over this region of Africa and that the differences with the measurements are acceptable. Both for the three stations near the Gulf of Guinea as well as for Brazzaville in Central Africa, the modelled seasonal cycle shows quite a high correlation with the measurements.

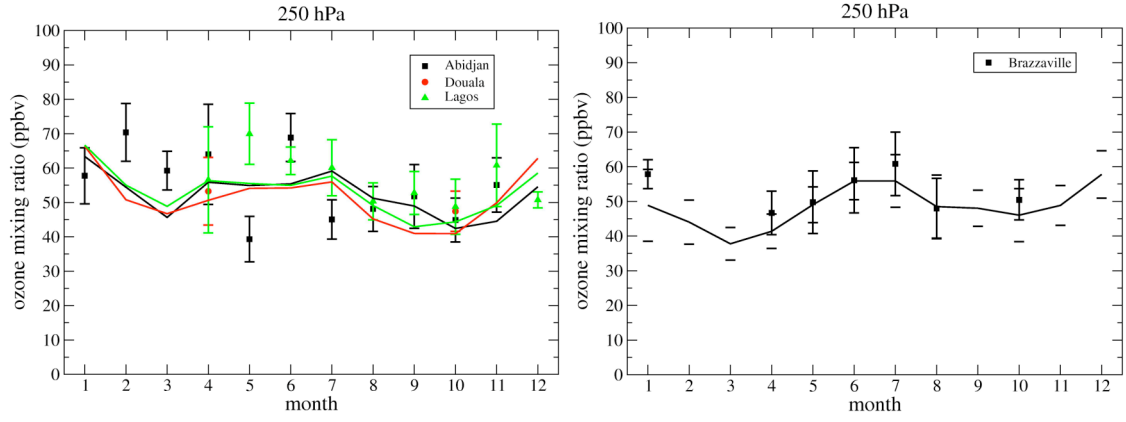

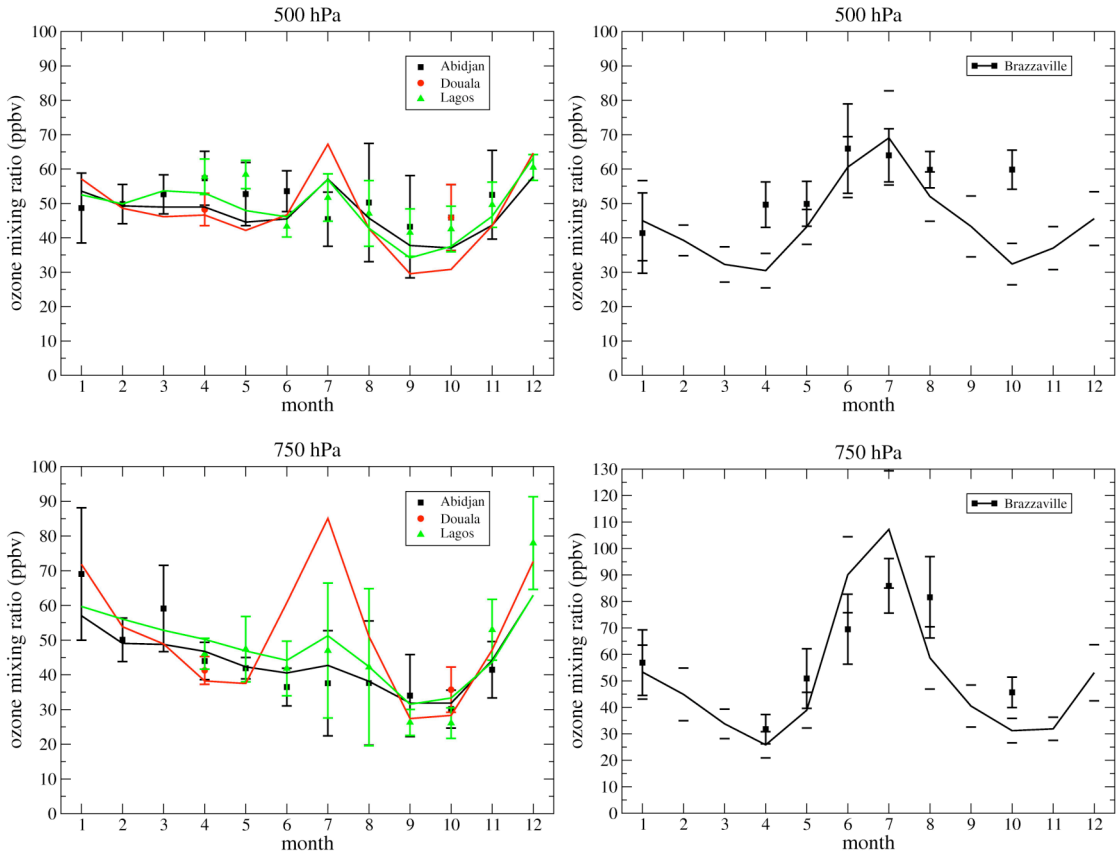

Figure 21. Seasonal cycles in O_3 mixing ratios at 250, 500 and 750 hPa for the year 2000. MOZAIC measurements (symbols) are compared with model results based on the RETROv1 emissions (lines).

Tropospheric burdens and budgets

The TM4 model has also been used to analyse the tropospheric budget of ozone (O_3) and burden of carbon monoxide (CO) on a monthly basis assuming a fixed tropopause height during each month, defined as the 150-ppbv level of the monthly mean ozone mixing ratio. The resulting annual budget terms for the year 2000 are given in Table 2 for the continental regions of West Africa and Northern and Southern Central Africa as well as for the Atlantic region around the Gulf of Guinea. Figures 22 and 23 show the corresponding monthly variations for the simulation using the GFEDv1 emissions (in combination with operational meteorological data) and the simulation using the RETROv1 emissions in combination with the ERA-40 reanalysis data.

Region	O_3 Production (Tg/yr)	O_3 Loss (Tg/yr)	O_3 Deposition (Tg/yr)	O_3 Influx (Tg/yr)	O_3 Burden (Tg)	O_3 Lifetime (days)	CO Burden (Tg)
West Africa	176.7 (170.0 / 165.7)	151.3 (155.4 / 149.1)	18.3 (16.6 / 16.3)	-7.1 (2.1 / -0.32)	5.91 (5.30 / 5.01)	12.8 (11.3 / 11.1)	7.55 (6.37 / 6.33)
Northern Central Africa	194.7 (198.7 / 191.2)	136.4 (144.2 / 141.2)	27.9 (26.5 / 26.2)	-30.4 (-28.5 / -23.8)	5.56 (4.98 / 4.80)	12.4 (10.7 / 10.5)	6.52 (5.76 / 5.76)
Southern Central Africa	198.3 (190.7 / 190.6)	134.3 (136.7 / 138.3)	29.6 (25.8 / 25.5)	-34.4 (-28.4 / -26.9)	5.27 (4.61 / 4.50)	11.8 (10.4 / 10.1)	7.13 (5.63 / 5.96)
Atlantic region	120.1 (127.2 / 130.3)	117.3 (123.4 / 123.2)	7.25 (6.58 / 6.25)	4.51 (2.78 / -0.87)	6.12 (5.44 / 5.30)	18.0 (15.3 / 15.0)	6.71 (5.75 / 5.83)

Table 2. Tropospheric ozone budget, burden and lifetime and tropospheric CO burden for the year 2000 calculated in the TM4 model. The first value corresponds to the simulation using the GFEDv1 emissions and operational meteorological data; the values in parentheses correspond to the simulations based on the RETROv1 emissions, using the ERA-40 / operational meteorological data.

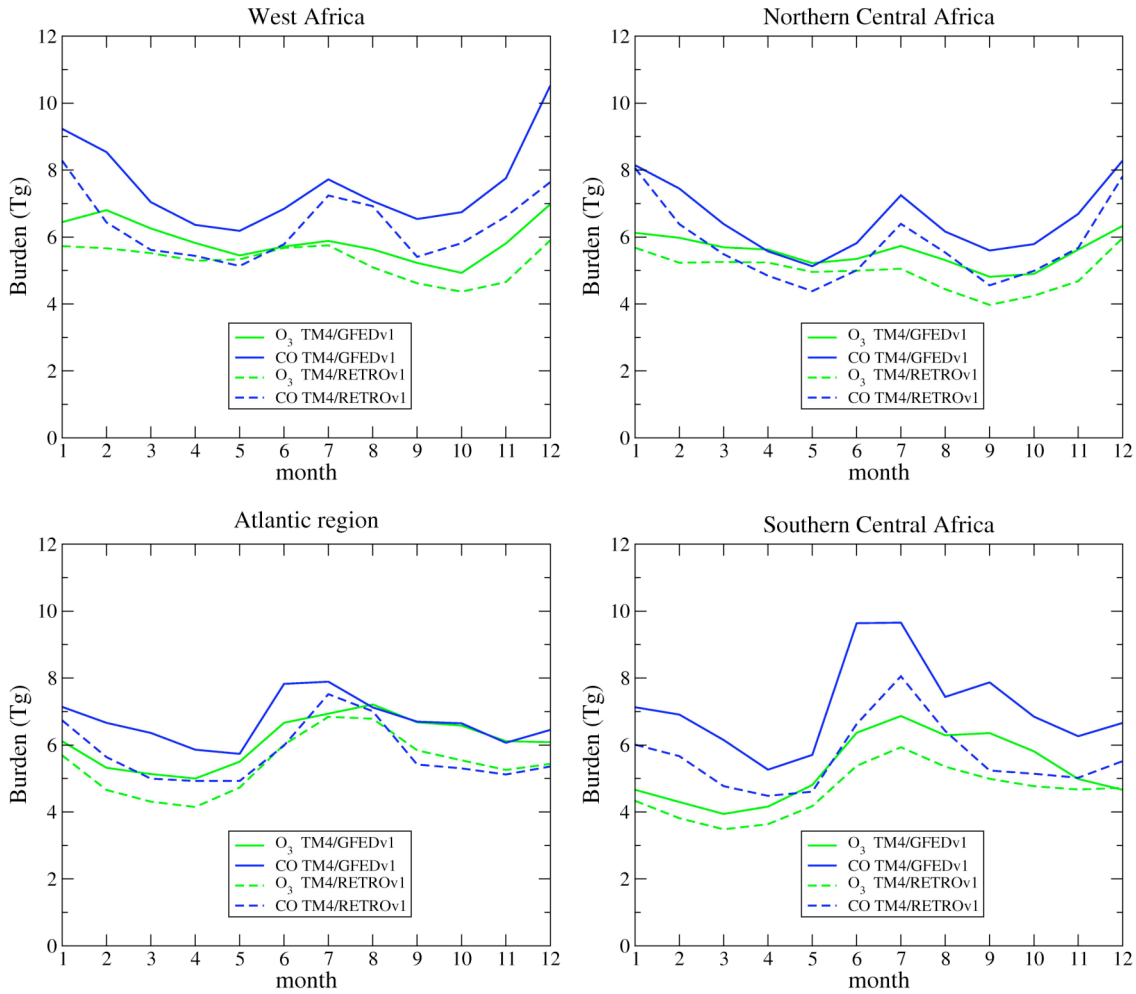

Figure 22. Seasonal cycles in tropospheric O_3 and CO burdens for the year 2000 from TM4 simulations using the GFEDv1 and the RETROv1 emissions.

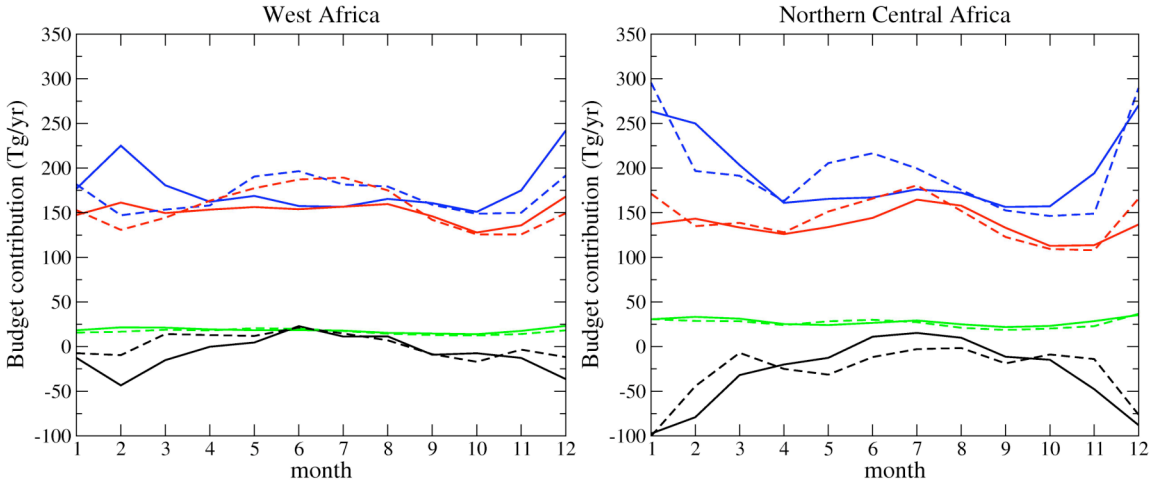

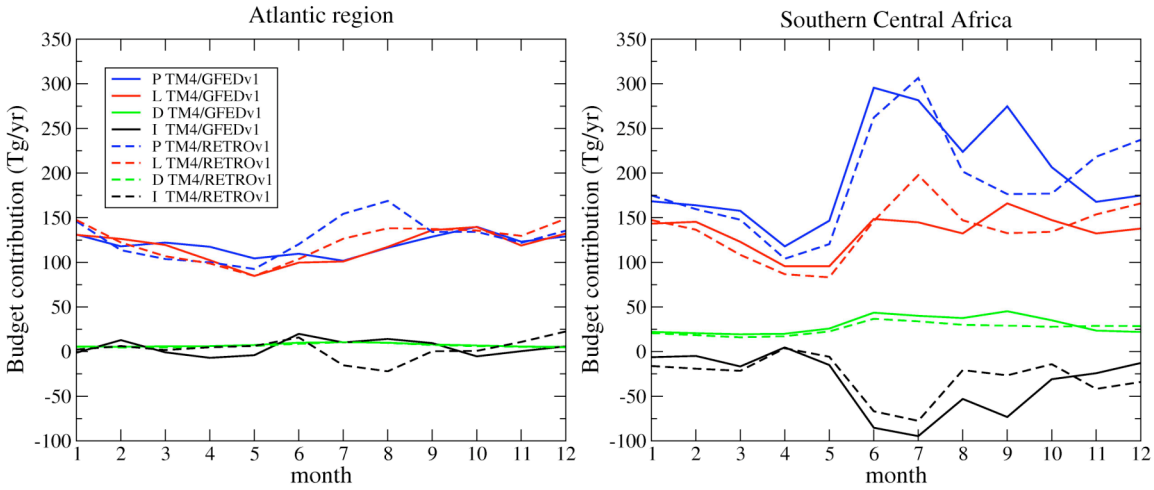

Figure 23. Seasonal cycles in the tropospheric O_3 chemical production (P), chemical loss (L), deposition (D), and regional influx (I) for the year 2000 from TM4 simulations using GFEDv1 and the RETROv1 emissions.

4. Aerosols over West Africa

Besides their impact on the radiative and climatic budget of the atmosphere, aerosols over West Africa play an important role in the cycling of atmospheric compounds through heterogeneous reactions between gases and particles - IDAF measurements of wet deposition in the wet and dry savannas of West Africa show for instance strong interactions between terrigeneous particles and nitrogeneous compounds (Yoboué et al., 2005). Aerosols over West Africa are a mixture of mineral dust from the Sahara and Sahel region, biomass/domestic/fossil fuel burning aerosols, conversion of VOC produced by vegetation and anthropogenic activities into secondary organic aerosols (SOA), and sulphate coming from oceans and urban/industrial regions. Aerosol budgets studies are presented here in order to quantify the different components of the aerosol budget over West Africa. The TM4 model has been used to assess biomass burning emissions, especially black carbon budget and the role of secondary organic aerosol. Dust budgets have been calculated based on an analysis of MODIS. Whilst not a modelling study in itself, these results can be used within AMMA to validate aerosol optical depths simulated by the models.

a) Carbonaceous Aerosols

Biomass burning emission inventories for gases, black carbon (BC), primary organic carbon and total organic carbon particles) have been derived for 2000 from burnt areas given by Spot vegetation satellite and appropriate emission factors. Differences with the older inventories are important (see Figure 24 for the monthly differences in black carbon emission when considering Liousse et al., 1996 (called old inventory) and new emission inventory for 2000). This shows the need for the models to run with emissions obtained from satellite burnt areas of the right year and not just inventories based on fire counts. In AMMA program, inventories will derived for the year 2005, 2006 and 2007 from Spot vegetation data. Emissions using this technique are also be derived for trace gases as well as aerosols (WP2.4.3).

New global emission inventories for fossil fuel (traffic, industry...) and biofuel (domestic fires) combustions for the period 1860-2030 have also been derived recently. In this work (Junker and Liousse, 2006) both emission factors and United Nations fuel consumptions have been updated.

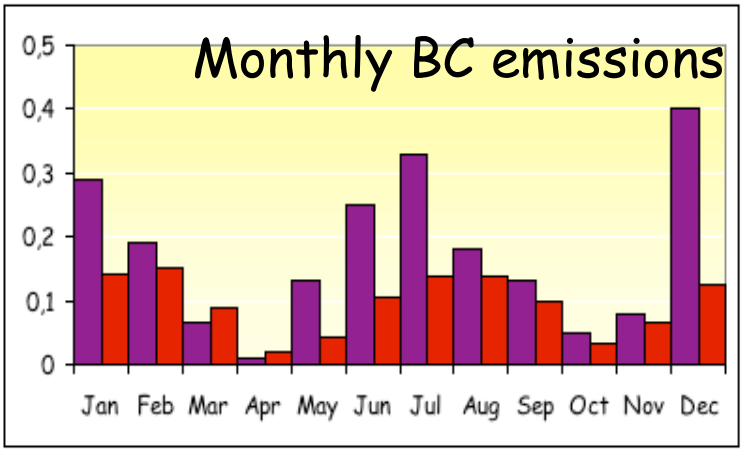

Figure 24. Seasonal variations of BC emissions in TgC/yr (red : old inventory, purple : new inventory for year 2000)

Evaluation of new biomass burning aerosol emission dataset

The TM4 model has been run for the year 2000 and compared to available BC data although only a few measurements exist near to biomass burning sources. Using available data at some of AMMA super-sites, gives a better agreement between the modelled and measured BC concentrations with the new emission inventories (not shown). For example, at Djougou during the dry season, concentrations are increased by 86% with the new biomass burning inventory and by 54% at Banizoumbou. Outside the dry season, there is also a large impact of biofuel sources on BC concentrations.

The new aerosol emission inventories have also been included in RegCM3 with a zoom on Africa and simulations performed for the year 2000 to see the impact on aerosol burden, deposition and radiative impacts. This model version includes sulphate and carbonaceous aerosols. Figure 25 shows some preliminary results. Aerosol optical depths obtained by the model with the new biomass burning emissions compare better with MODIS data in July 2000 than runs with the old inventories over biomass burning regions in central Africa. Clearly dust aerosols are also contributing to optical depths further north over West Africa (see next section)

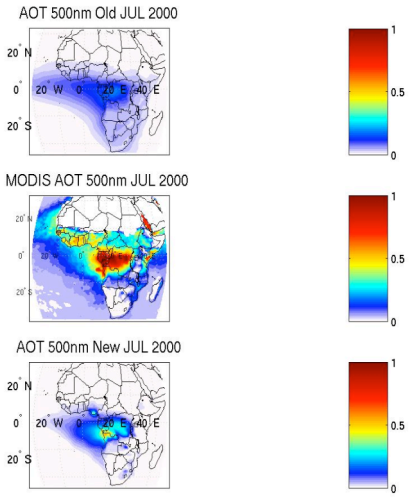

Figure 25. RegCM3 AOT as simulated with the old and new inventory in comparison with MODIS AOT at 500 nm

Organic aerosol budget

First results of global distributions of secondary organic aerosol of anthropogenic origin (SOAAc), secondary organic aerosol of biogenic origin (SOABc), primary organic carbon (OCp) obtained with ORISAM-TM4 model are presented in Figures 26, 27 and 28 for August. The distribution of total organic carbon particles (OCtot) calculated from these maps has also been added. With the set of precursors and the inventories for gases and particles included in the model, the model shows the relative importance of primary organic particles in the global OCt budget during the dry season above the biomass burning events. Also, the importance of biogenic secondary organic aerosol in the other areas should be noted; this fraction is higher than anthropogenic secondary organic aerosol fraction. A slight overestimate of SOAB is apparent in some places probably due to model chemistry scheme and the biogenic VOC emissions that have been used. Sensitivity studies are ongoing on these questions focusing on gaseous precursors/primary organic emissions and secondary organic aerosol conversions).

Figure 3 : OCt : ORISAM-TM4 August

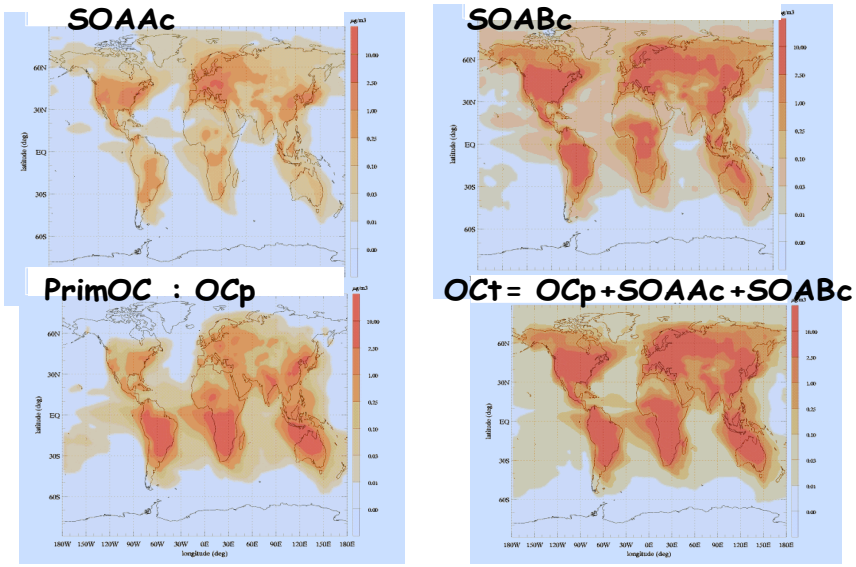

Figure 26. Results from ORISAM-TM4 for August in micro g per cm^3 (see text for details).

The OCt obtained with ORISAM-TM4 has also been compared with OCt from the TM4 tracer model by multiplying global distribution of OCp by a constant factor (methodology used up to now, see Liousse et al., 1996) (see Figure 27). The tracer model run without the conversion of SOA generally underestimates values of OCt. For example, in Djougou, in August, (wet season), OCt are increased by 95% with ORISAM-TM4 model due to the SOAB produced from biogenic precursors. However, over biomass burning areas, OCt given by the tracer version is higher due to the important fraction of OCp and to the less important SOA

formation proposed by ORISAM-TM4 model.

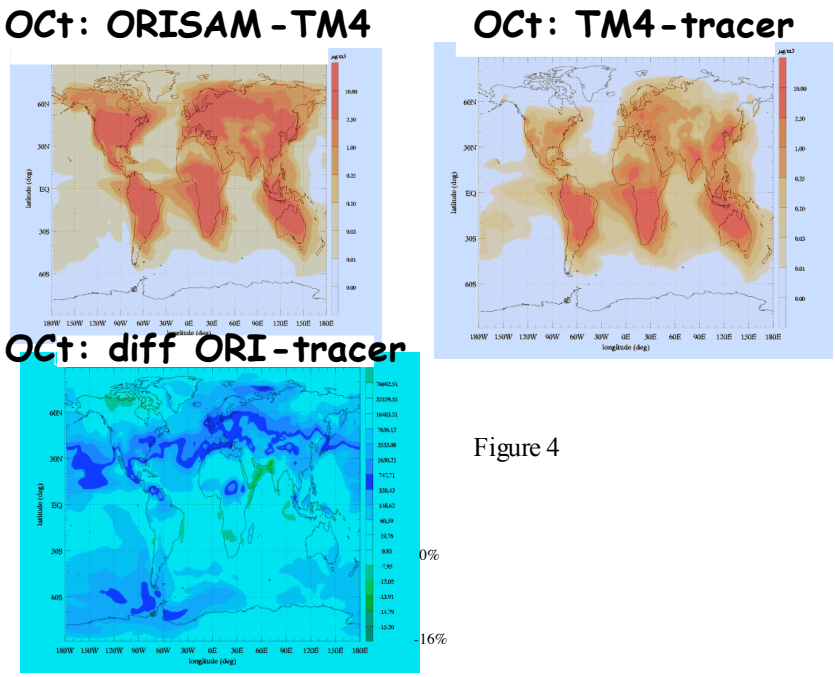

Figure 4

Figure 27. Comparison of results from ORISAM-TM4 and TM4-tracer (total organic aerosol) for August in micro g per cm^3 (see text for details).

The ratio OCp/OCtot is shown in Figure 29 for the two periods June, July, August and Dec, Jan, Feb. The results show that the ratio is variable (35-100%) and as previously described relative importance of primary particles from anthropogenic sources and formation of SOA from biogenic precursors can be retrieved. Such maps could be used in climate models without an aerosol module allowing the formation of SOA and avoiding the use of a constant factor of conversion between OCp and OCt globally.

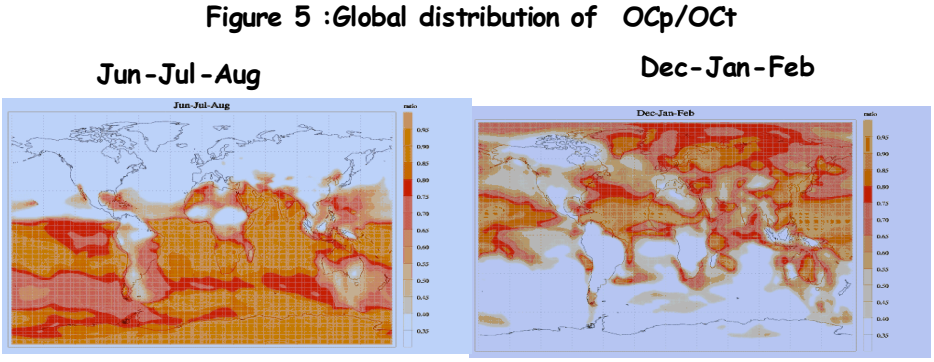

Figure 28. Global distribution of OCp/Oct for June/July/August (left) and Dec/Jan/Feb (right) – see text for details.

b) Mineral Dust

Here results from analysis of MODID satellite data are presented and comparisons with AERONET data since both these datasets are often used to validate both global and regional models (also related to work in 2.4). MODIS spectral radiances from 0.55 μm to 2.1 μm are used to derive aerosol characteristics over the oceans [*Tanré et al*., 1997]. The algorithm uses measured spectral radiances over cloud-free, glint-free ocean scenes, to derive the aerosol information by fitting it to a lookup table, that includes both fine aerosol (effective radius between 0.1, and 0.25 μm) and coarse aerosol (effective radius between 1 and 2.5 μm). The MODIS derived aerosol optical thicknesses are validated [*Remer et al.,* 2002], the aerosol optical thickness is derived with an error of $\Delta\tau = \pm 0.03 \pm 0.05\tau$, against AERONET data. The aerosol optical thickness τ derived from MODIS over ocean is composed of maritime, τ_{ma}, dust, τ_{du}, and anthropogenic, τ_{an}, aerosol (biomass burning and urban industrial pollution):

$$\tau = \tau_{ma} + \tau_{du} + \tau_{an} \quad (1)$$

The second parameter f, that is derived, is the contribution of the fine aerosol to the optical thickness. For a mixture of dust, maritime aerosol and anthropogenic aerosol, it is written:

$$f = [f_{ma}\tau_{ma} + f_{du}\tau_{du} + f_{an}\tau_{an}]/\tau \quad (2)$$

So, MODIS provides 2 measurements - τ and f and there are 6 unknowns: f_{ma}, τ_{ma}, f_{du}, τ_{du}, f_{an} and τ_{an}. We determine the fraction of fine aerosol for each of the aerosol types using MODIS aerosol measurements in regions of (i) concentrated dust, (ii) concentrated smoke, and (iii) mostly maritime aerosol in the Southern Atlantic (0-30°S). The results are:

$$f_{ma}=0.3\pm0.1,\ f_{du}=0.5\pm0.05 \text{ and } f_{an}=0.9\pm0.05 \quad (3)$$

We do not have a mechanism to distinguish dust from maritime aerosol in the MODIS data therefore the maritime aerosol optical thickness is estimated independently from the MODIS measurements. In remote areas, with little contamination of the maritime atmosphere we found that on average $\tau_{ma} = 0.06\pm0.005$, in agreement with an analysis of baseline maritime aerosol [*Kaufman et al*. 2001]. Finally, the dust optical thickness, τ_{dust} is derived from:

$$\tau_{dust} = [\tau(f_{an}-f)-\tau_{ma}(f_{an}-f_{ma})]/(f_{an}-f_{du}) \quad (4)$$

As an additional validation, we show in Figure 29 for the Capo Verde AERONET station, which is on the path of African dust, a comparison between MODIS inversion and sun-photometer measurements.

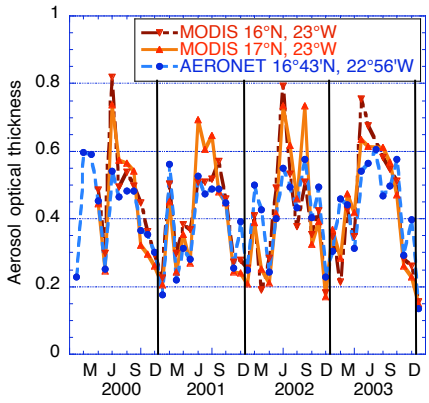

Figure 29. Monthly averages of the aerosol optical thickness measured by AERONET in Capo Verde and derived from MODIS around the location of the sunphotometer over the ocean (extracted from Kaufman et al., 2005).

For the 3 full years of operation the MODIS optical thickness was 0.40-0.42 and AERONET was 0.39-0.43. The MODIS data are from Terra at ~ 10:30 am local time, the AERONET data are averaged on the daily hours. The AERONET level 1.0 data are used with only partial cloud screening due to possible screening of heavy dust with the accompanied clouds. Both data sets show similar seasonal cycle of the aerosol with maximum in the June-Sept time frame. In Figure 30, we report maps of optical thickness for the 3 years near the African coast. They have very similar behaviour although year 2001-2002 looks a less dusty near. These results can be used to compare to global (and regional) model simulations in AMMA.

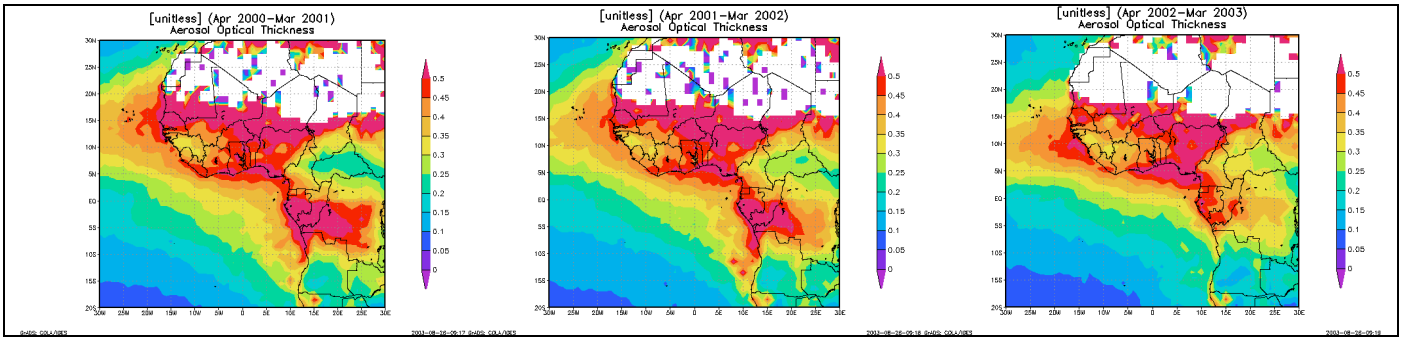

Figure 30: Yearly averages of the optical thickness from April to May, in 2000-2001(left), 2001-2002 (middle) and 2002-2003 (right) – note different scale to Figure 25.

Analysis of MODIS observations have also been used to show that, in contrast to previous lower estimates, approximately 240 +/- 80 Tg dust are transported annually over the Atlantic Ocean and that 140 +/- 40 Tg dust are deposited in the Atlantic Ocean (Kaufman et al., 2005). Out of this 50 Tg fertilizes the Amazon Basin – this is four times previous estimates and help to explain previous paradox regarding the sources of nutrition to the Amazon Basin. These results compare favourably with dust transport models (e.g. GOCART) and show the first example of the quantitative use of MODIS aerosol data.

5. Conclusions

The previous sections have shown some of the first evaluations of global models participating in the AMMA project against available data. The aim of this report is to highlight the key uncertainties in the models and to make recommendations about priorities for future work in the project. Several key processes have been identified which in general correspond well with

the objectives of 2.4 which focuses on detailed process studies using the data collected during the EOP and SOPs. The following are recommended as priorities:

- ***Emissions*** – improved emission inventories being developed within the AMMA project, particularly on soil NO_x and biomass burning in 2.4.3 should be incorporated into the global (and regional) models when available. It will also be important to link studies planned in 2.4.4 (and 1.1.2) on lightning NO_x to global scale studies and improvements in the parameterisations used currently often based on convective cloud top height. Whilst, satellite column data can be used to evaluate model emissions, differences between retrieval techniques also need to be examined in greater detail over the West African region.

- ***Transport*** - tracer transport schemes used in global models, especially for deep convection and boundary layer exchange require further evaluation. This work should be closely linked to studies planned using the transport only version of models and work with higher resolution regional and cloud resolving models (4.1) and could include specially designed tracer experiments. Model results and subsequent O_3 production are highly dependent on the vertical redistribution of O_3 precursors such as NO_x, VOCs and CO as well as subsequent horizontal advection. The import of O_3 and its precursors from other regions (Europe (mid-troposphere), central Africa (low-mid troposphere), India (upper troposphere, TTL)) should also be considered especially during the wet season.

- ***Chemistry*** – the O_3 production potential of air masses is a key uncertainty in global models and depends on many factors – assessment of contributing processes on a case study basis (2.4.2 and 2.4.4) should feed into improvements in the global models. Highly uncertain processes relate to the nitrogen budget – washout of HNO_3, heterogeneous loss on mineral dust, lightning emissions. Degradation schemes for VOCs emitted from biogenic sources need better evaluation.

- ***Aerosols*** – the factors influencing aerosol composition are still very uncertain and as shown here, carbonaneous aerosols can make a significant contribution to aerosol optical depths over burning regions followed by possible transport into West Africa. The interactions between aerosols and chemistry are also important particularly in the formation of SOA and the uptake of HNO_3 on mineral dust.

References

Andreae, M. O., and P. Merlet, Emission of trace gases and aerosols from biomass burning, *Global Biogeochem. Cycles*, 15(4), 955–966, doi:10.1029/2000GB001382, 2001.

Dentener, F., Stevenson, D., Cofala, J., Mechler, R., Amann, M., Bergamaschi, P., Raes, F., and Derwent, R. The impact of air pollutant and methane emission controls on tropospheric ozone and radiative forcing: CTM calculations for the period 1990-2030, *Atmos. Chem. Phys.,*5, 1731-1755, SREF-ID:1680-7324/ap/2005-5-1731, 2005.

Galy-Lacaux, C., A. I. Modi, Precipitation Chemistry in the Sahelian savanna of Niger, Africa, *J. Atmos. Chem.* 30: 319-343, 1998.

Guillaume, B., et al., , in review, *Tellus(B)*, 2006.

Hauglustaine, D.A., et al., 2004: Interactive chemistry in the Laboratoire de Météorologie dynamique general circulation model: Description and background tropospheric chemistry evaluation. *J. Geophys. Res.*, vol. 109, D04314, 2004.

Jaeglé, L., R.V. Martin, K. Chance, L. Steinberger, T.P. Kurosu, D.J. Jacob, A.I. Modi, V. Yoboué, L. Sigha-Nkamdjou, and C. Galy-Lacaux, Satellite mapping of rain-induced nitric oxide emissions from soils, *J. Geophys. Res.,* 109, D21310, doi:10.1029/2004JD004787, 2004.

Junker, C. and C. Liousse, *Atmos. Phys. Chem. Discuss*., 2006.

Kaufman, Y. J., A. Smirnov, B. N. Holben and O. Dubovik, Baseline maritime aerosol: methodology to derive the optical thickness and scattering properties, *Geophys. Res. Lett.*, *28*, 3251-3254, 2001.

Kaufman, Y. J., I. Koren, L. A. Remer, D. Tanré, P. Ginoux, and S. Fan, Dust transport and deposition observed from the Terra-Moderate Resolution Imaging Spectroradiometer (MODIS) spacecraft over the Atlantic Ocean, *J. Geophys. Res.*, *110*, D10S12, doi:10.1029/2003JD004436, 2005.

Kleidman, R. G., N. T. O'Neill, L. A. Remer, Y. J. Kaufman, T. F. Eck, D. Tanré, O. Dubovik, and B. N. Holben, Comparison of Moderate Resolution Imaging Spectroradiometer (MODIS) and Aerosol Robotic Network (AERONET) remote-sensing retrievals of aerosol fine mode fraction over ocean, *J. Geophys. Res*., 110, D22205, doi:10.1029/2005JD005760, 2005.

Konaré, A., et al., submitted to *Tellus B*, 2006.

Liousse, C., B. Guillaume, J.M Grégoire, A. Konaré, F. Solmon, C. Galy, A. Mariscal, D. Laouali, and C. Junker, Impact of African biomass burning emissions on combustion aerosol burden, transport and deposition, to be submitted, 2006.

Marenco, A., et al. (1998), Measurement of ozone and water vapour by Airbus in-service aircraft: The MOZAIC airborn program, an overview, *J. Geophys. Res*., 103, 25, 631-25, 642.

Olivier, L. G. J., and J. J. M. Berdowski, Global emission sources and sinks, in *The Climate System,* edited by J. Berdowski, R. Guicherit, and B. Heij, pp. 33-77, Swets and Zeitlinger B. V., Lisse, Netherlands, 2001.

Olivier, J.G.J., Bouwman, A.F., Van der Maas, C.W.M., Berdowski, J.J.M., Veldt, C., Bloos, J.P.J., Visschedijk, A.J.H., Zandveld, P.Y.J. and Haverlag, J.L. Description of EDGAR Version 2.0: A set of global emission inventories of greenhouse gases and ozone-depleting substances for all anthropogenic and most natural sources on a per country and on 1°´1°grid. *RIVM Rep 77060002/TNO MEP report nr. R96/119,* RIVM, Bilthoven, The Netherlands, 1996.

Pradier S., J.L. Attié, M. Chong, J. Escobar, V-H. Peuch, J-F Lamarque, B. Kattatov, D. Edwards, Evaluation of 2001 springtime CO transport over West Africa using MOPITT CO measurements assimilated in a global chemistry transport model. *Tellus,* in press, 2006.

Price, C., J. Penner, and M. Prather (1992), A simple lightning parametrization for calculating global lightning distributions, *J. Geophys. Res.*, 97, 9919-9933.

Remer, L. A., D. Tanré, Y. J. Kaufman, et al., Validation of MODIS aerosol retrieval over ocean. *Geophys. Res. Lett*., 29 (12): art. no. 1618 JUN 15, 2002

Sauvage, B., V. Thouret, J.-P. Cammas, F. Gheussi, G. Athier, and P. Nédélec, Tropospheric ozone over Equatorial Africa: regional aspects from the MOZAIC data, *Atmos. Chem. Phys*., 5, 311–335, 2005.

Schultz, M.G, A. Heil, J.J. Hoelzemann, A. Spessa, K. Thonicke, J. Goldammer, A.C. Held, J.M. Pereira (2005), Global emissions from wildland fires from 1960 to 2000, *Global Biogeochem. Cycles*, submitted, 2005.

Tanré, D., M. Herman and Y.J. Kaufman,, Information on aerosol size distribution contained in solar reflected radiances. *J. Goephys. Res.*, *101*, 19043-19060, 1996.

Tanré, D., Y. J. Kaufman, M. Herman and S. Mattoo, Remote sensing of aerosol over oceans from EOS-MODIS, *J. Geophys. Res, 102*, 16971-16988. 1997.

van der Werf, G.R., J.T. Randerson, G.J. Collatz, and L. Giglio, Carbon emissions from fires in tropical and subtropical ecosystems, *Global Change Biology*, 9, 547–562, 2003.

Van der Werf, G.R., J.T. Randerson, G.J. Collatz, L. Giglio, P. Kasibhatla, A. Arellano, S. Olsen, and E.S. Kasischke, Continental-scale partitioning of fire emissions during the 1997 to 2001 El Niño/La Niña period, *Science*, 303: 73-76, 2004.

van Noije, T.P.C., et al., Multi-model ensemble simulations of tropospheric NO_2 compared with GOME retrievals for the year 2000, *Atmos. Chem. Phys. Disc*., 6, 2965–3047, 2006.

Yienger, J.J., and H. Levy, II, Global inventory of soil-biogenic NO_x emissions, *J. Geophys. Res*., 100, 11,447–11,464, 1995.

Yoboué, V., C. Galy-Lacaux, J. P. Lacaux and S.Silué: Rainwater Chemistry and Wet Deposition over the wet Savanna Ecosystem of Lamto (Cote d'Ivoire). *J. Atmos. Chem.,* 52: 117-141, 2005.

Van der Werf, G.R., J.T. Randerson, G. J. Collatz, L. Giglio. 2003. Carbon emissions from fires in tropical and subtropical ecosystems. *Global Change Biology*. 9(4): 547-562. Copyright 2003 Blackwell Science.

Acknowledgements

We thank all the groups that have provided data shown in this report, especially MOZAIC data (Nedelec, Cammas – CNRS-LA), IDAF data (Galy-Lacaux – CNRS-SA), GOME data (KNMI/BIRA), MOPITT data (CNRS-LA, NCAR), MODIS and AERONET.